

Nano-Kirigami and strain physics in 2D materials

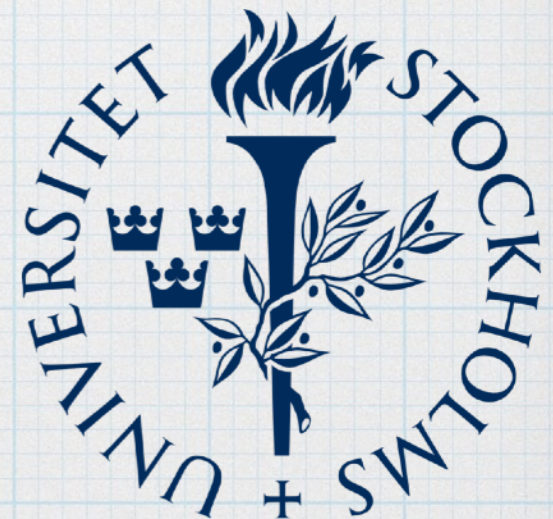
Habib Rostami

NORDITA

Stockholm, Sweden



2021, Feb 2ed
Nordita, Stockholm University

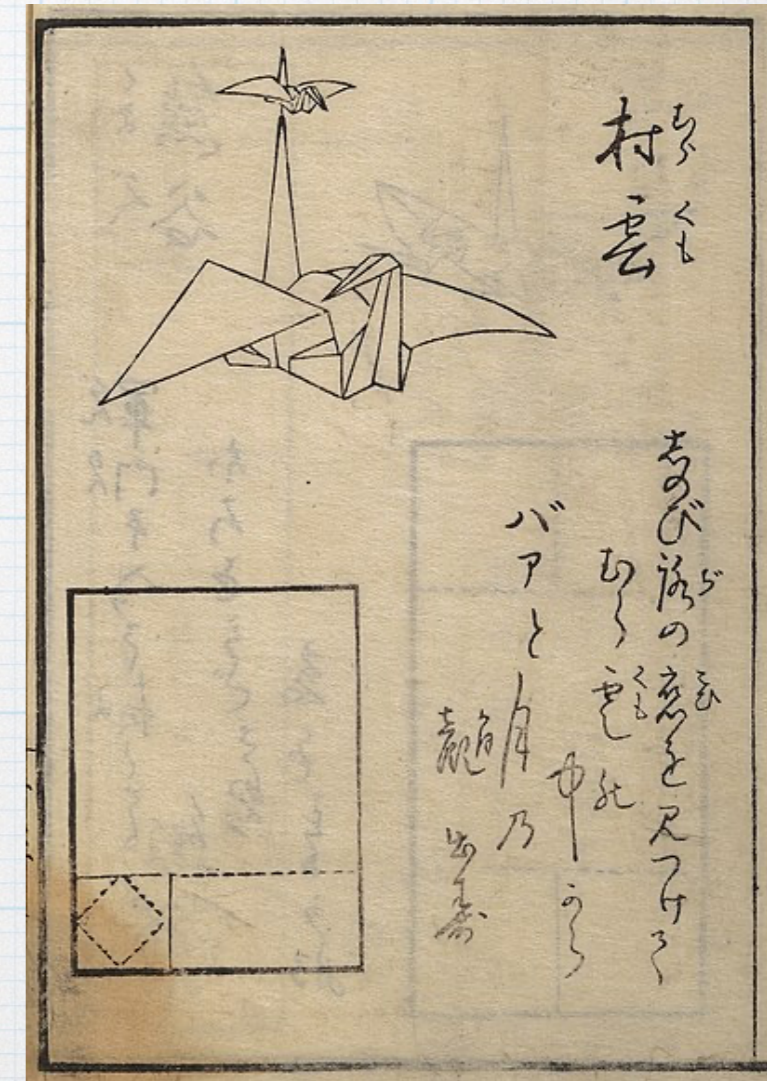


Origami (Paper folding)

The word 'origami' consists of two Japanese characters - ori, which means 'bend' or 'fold' and kami, that is 'paper.'



Wikipedia



Wikipedia: The folding of two origami cranes linked together, from the first known book on origami, *Hiden senbazuru orikata*, published in Japan in 1797

Kirigami (cutting and folding)

Google Kirigami

Marc Hagan-Guirey uses kirigami to ...
dezeen.com

Kirigami patterns, Origami architecture ...
pinterest.com

Marc Hagan-Guirey uses kirigami to ...
dezeen.com

☆ Origamic Architecture Instructions ...
pinterest.se

3d building | pop up card | paper art ...
youtube.com

FRANK LLOYD WRIGHT
PAPER MODELS
14 KIRIGAMI BUILDINGS TO CUT AND FOLD

Frank Lloyd Wright Pap...
archdaily.com

origamikirigami: Kirigami Architecture
pearlkirigami.blogspot.com

☆ Origamic Architecture Instructions ...
discover.hubpages.com

Kirigami - Wikipedia
en.wikipedia.org

Origami architecture
nl.pinterest.com

Kirigami: 7 amazing artworks made ...
mag.lexus.co.uk

Marc Hagan-Guirey uses kirigami to ...
dezeen.com

Kinetic Art #1 | Parametric House
parametrichouse.com

3D Popup Kirigami postcards on Behance
behance.net

Origamic Architecture – Gnarly Design
gnarlydesign.io

Le Corbusier Paper Models, 10...
diohoria2shop.com · In stock

Stretchable and Foldable Silicon Integrated Circuits

[Science 320, 507 (2008)]

Aim: personal health monitors and other biomedical devices, that require extreme mechanical deformations

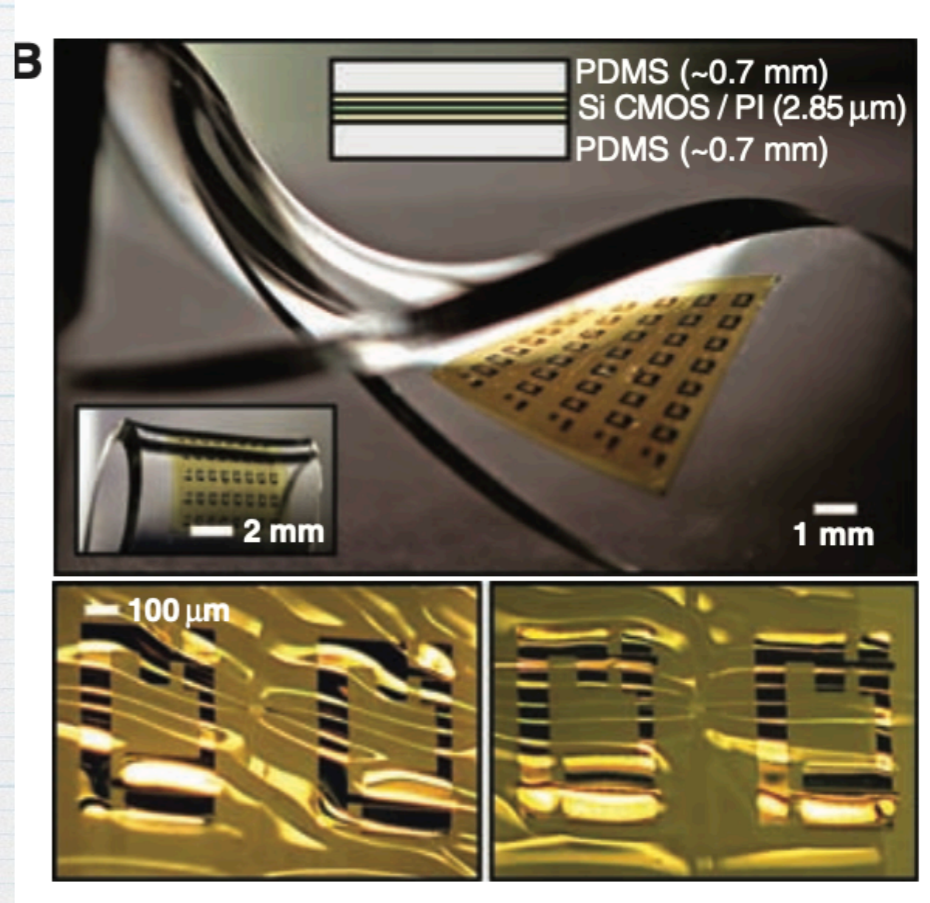
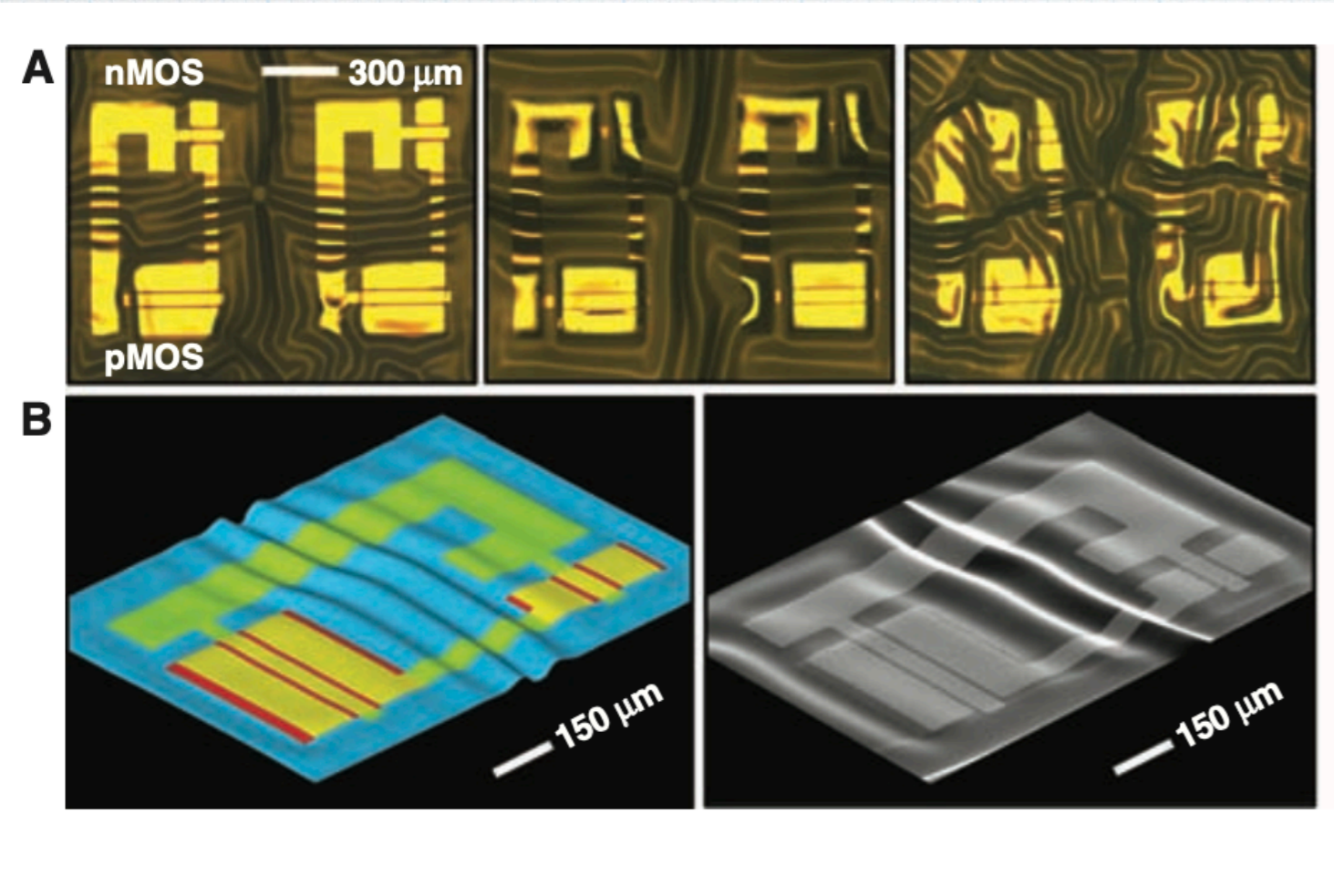
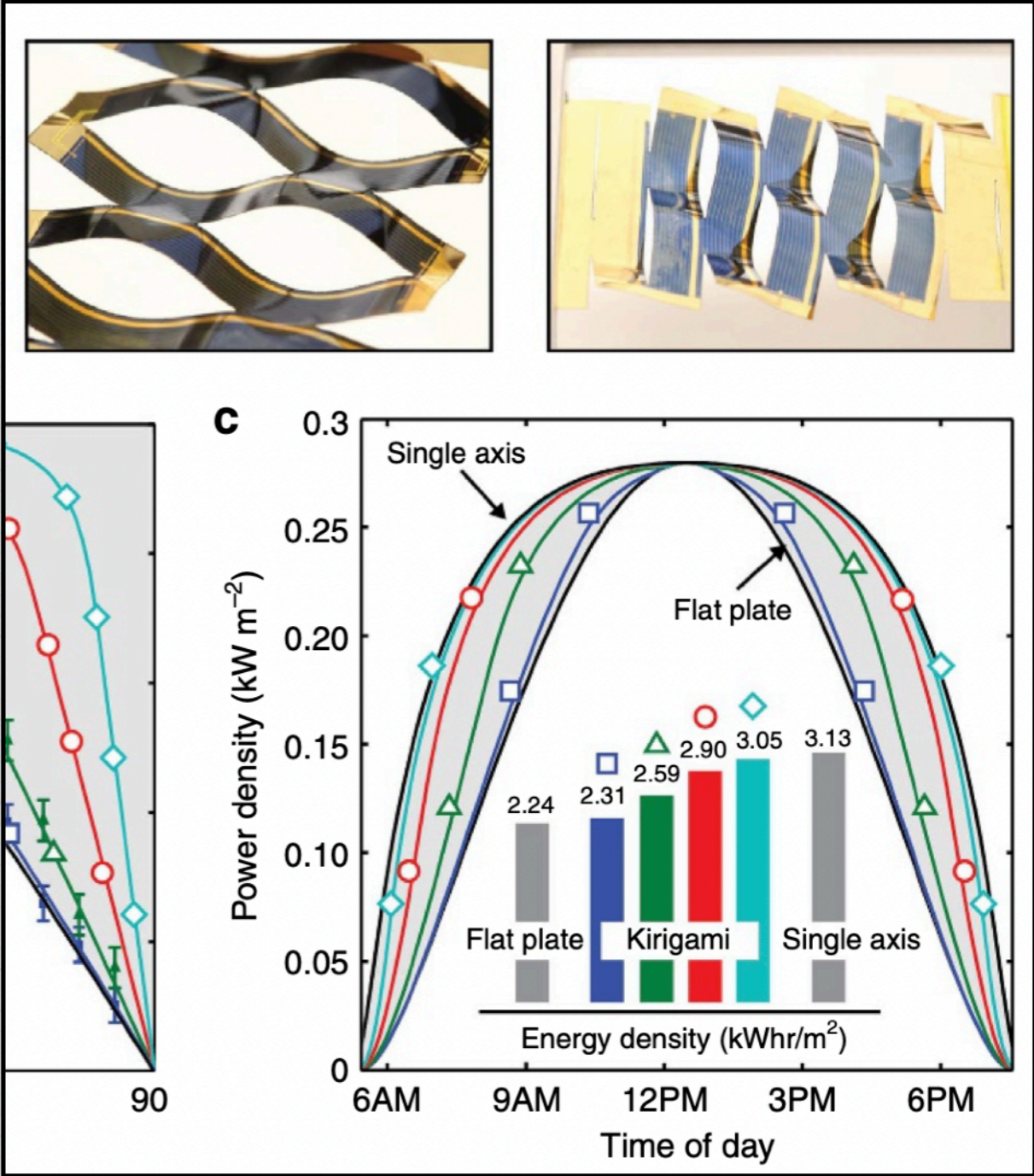
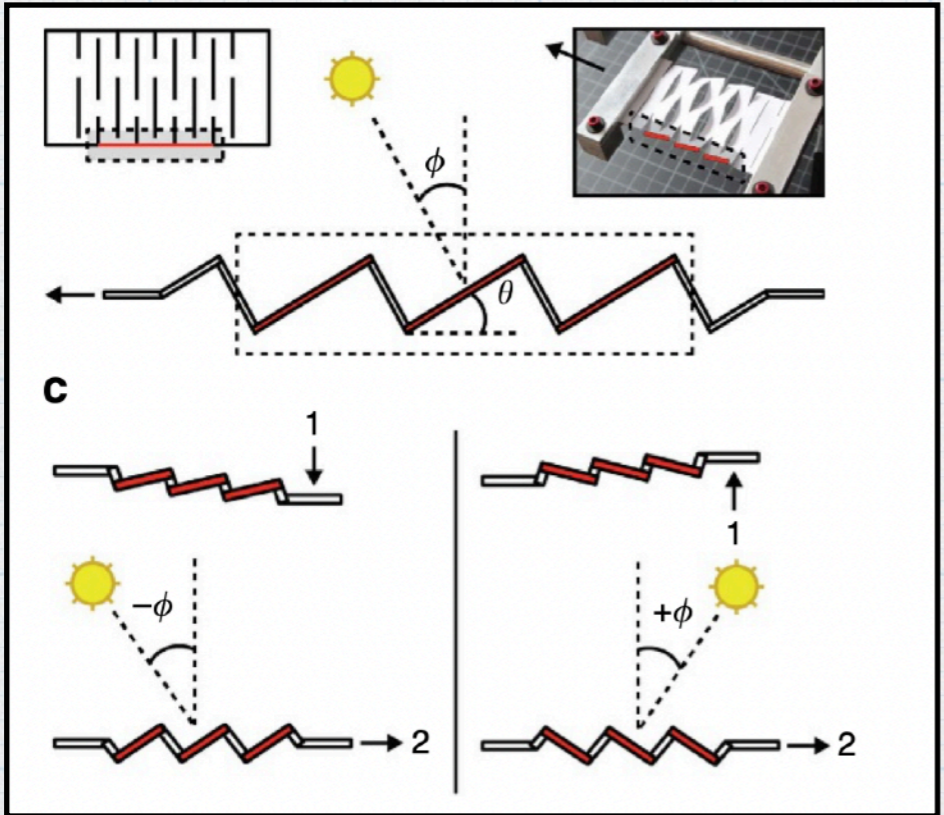
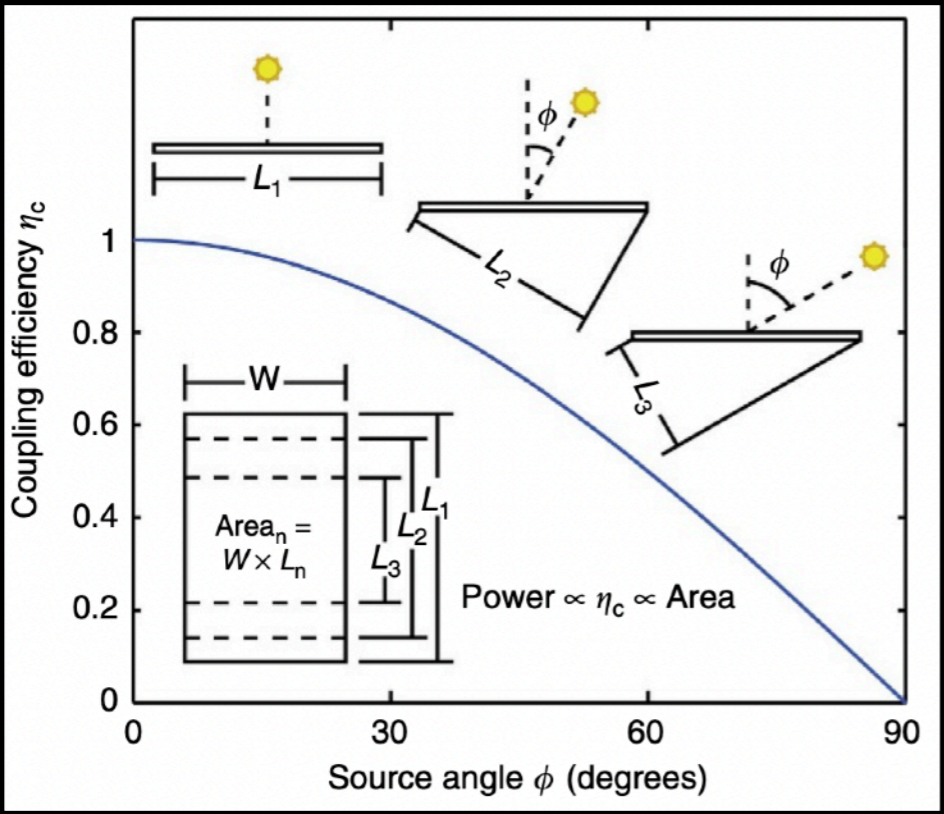


Fig. 2. (A) Wavy Si-CMOS inverters on PDMS, formed with various levels of prestrain. (left, $\epsilon_{pre} = 2.7\%$; center, $\epsilon_{pre} = 3.9\%$; right, $\epsilon_{pre} = 5.7\%$.) (B) Structural configuration determined by full 3D FEM of a system formed with $\epsilon_{pre} = 3.9\%$ (left) and perspective scanning electron micrograph of a sample fabricated with a similar condition (right). (C) Optical images of wavy Si-CMOS

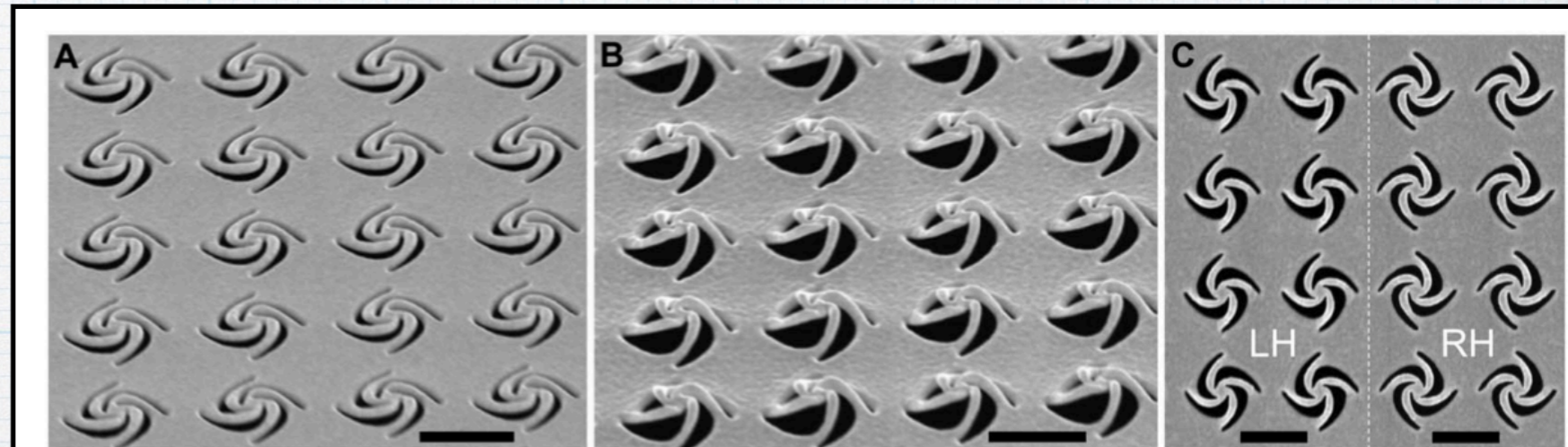
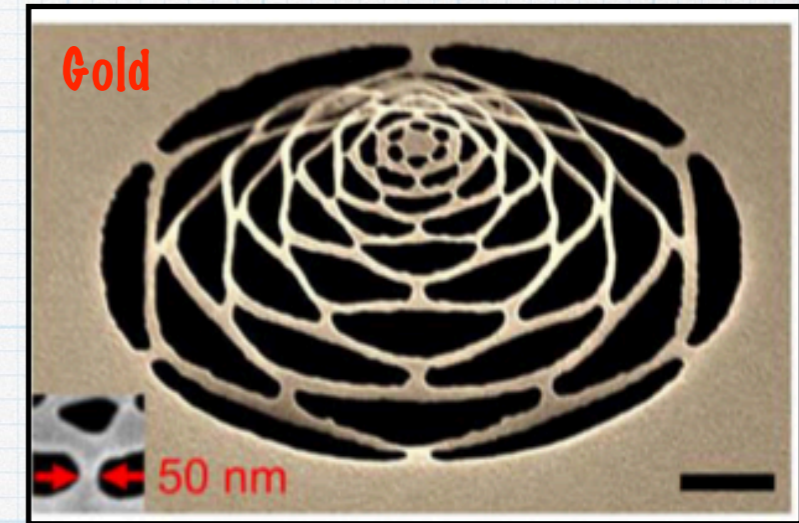
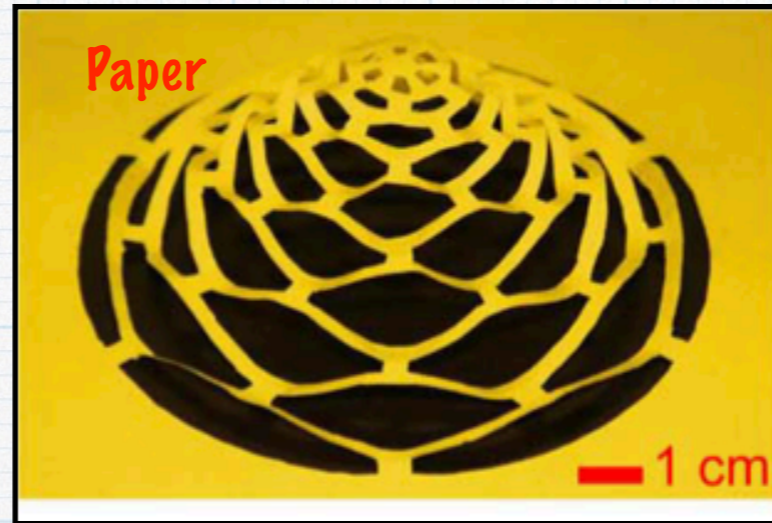
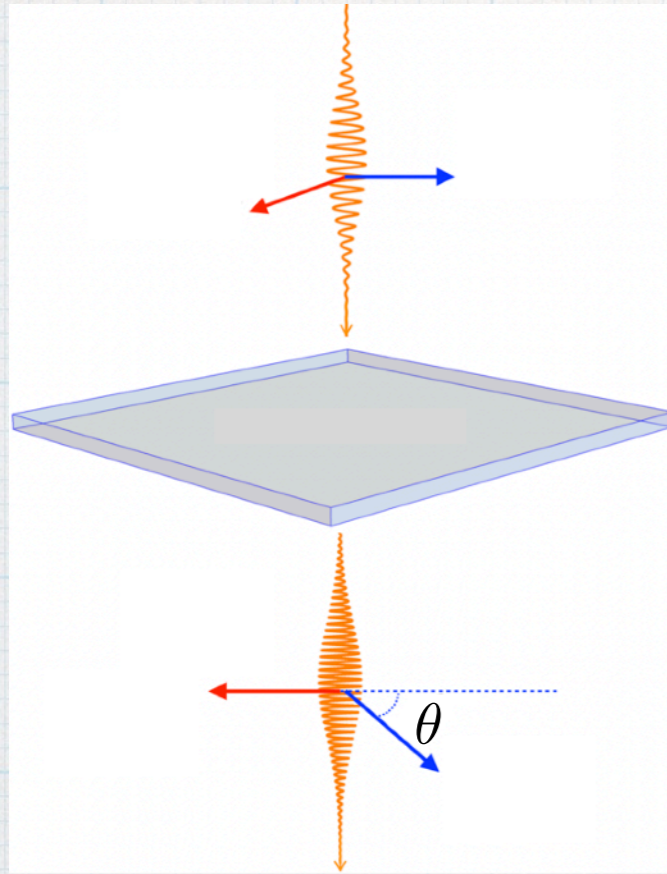
Dynamic kirigami structures for integrated solar tracking (GaAs Paper)



Nature Communications 6, 8092 (2015)

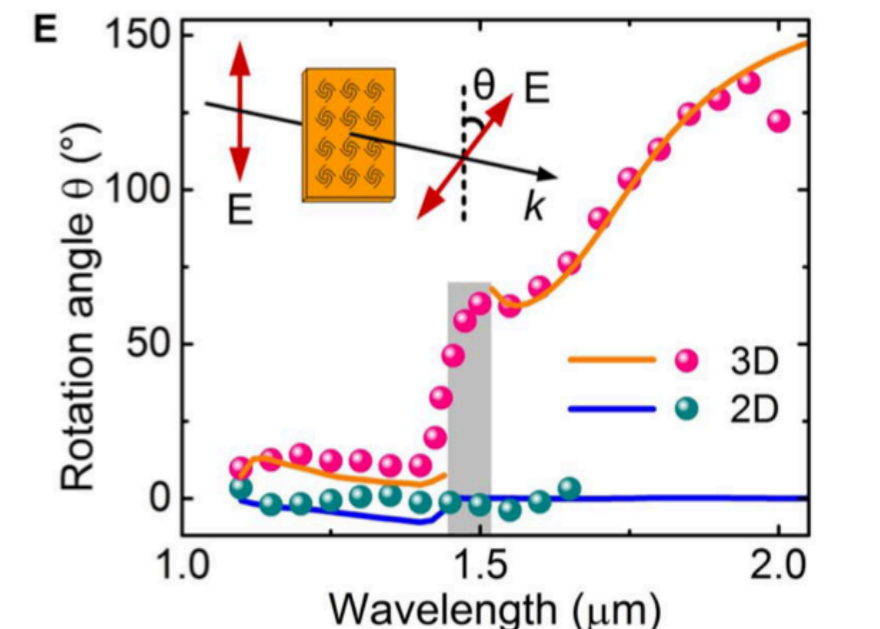
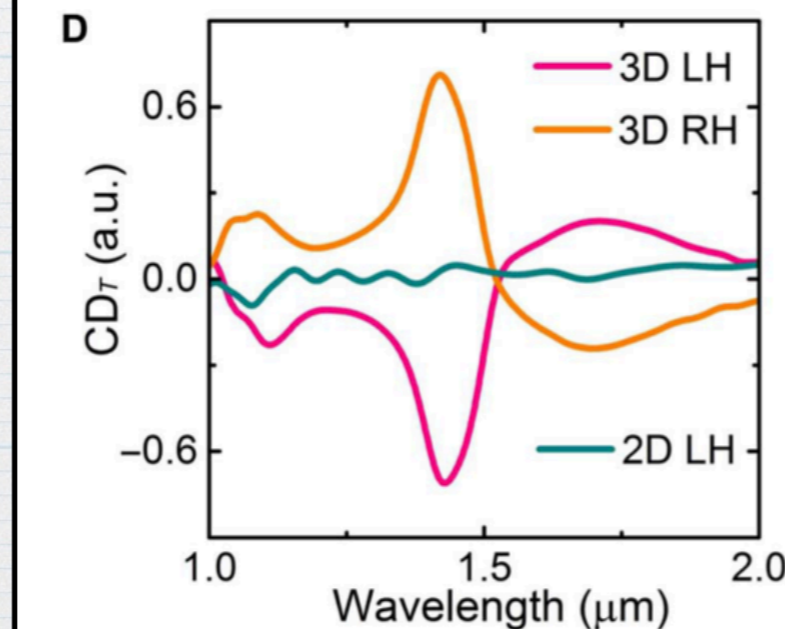
Nano-kirigami with giant optical chirality

Sci Adv 4 (7), eaat4436. (2018).



Circular Dichroism

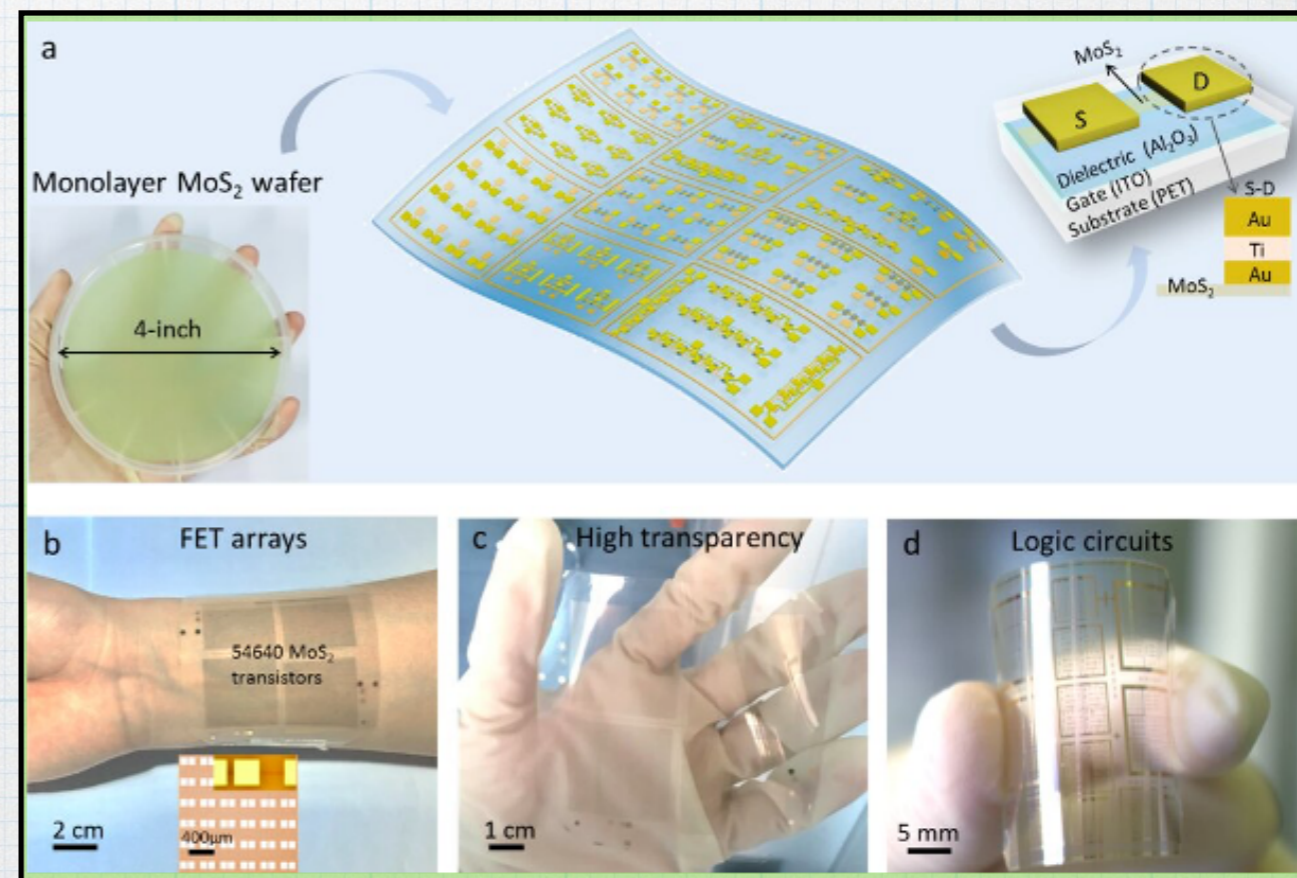
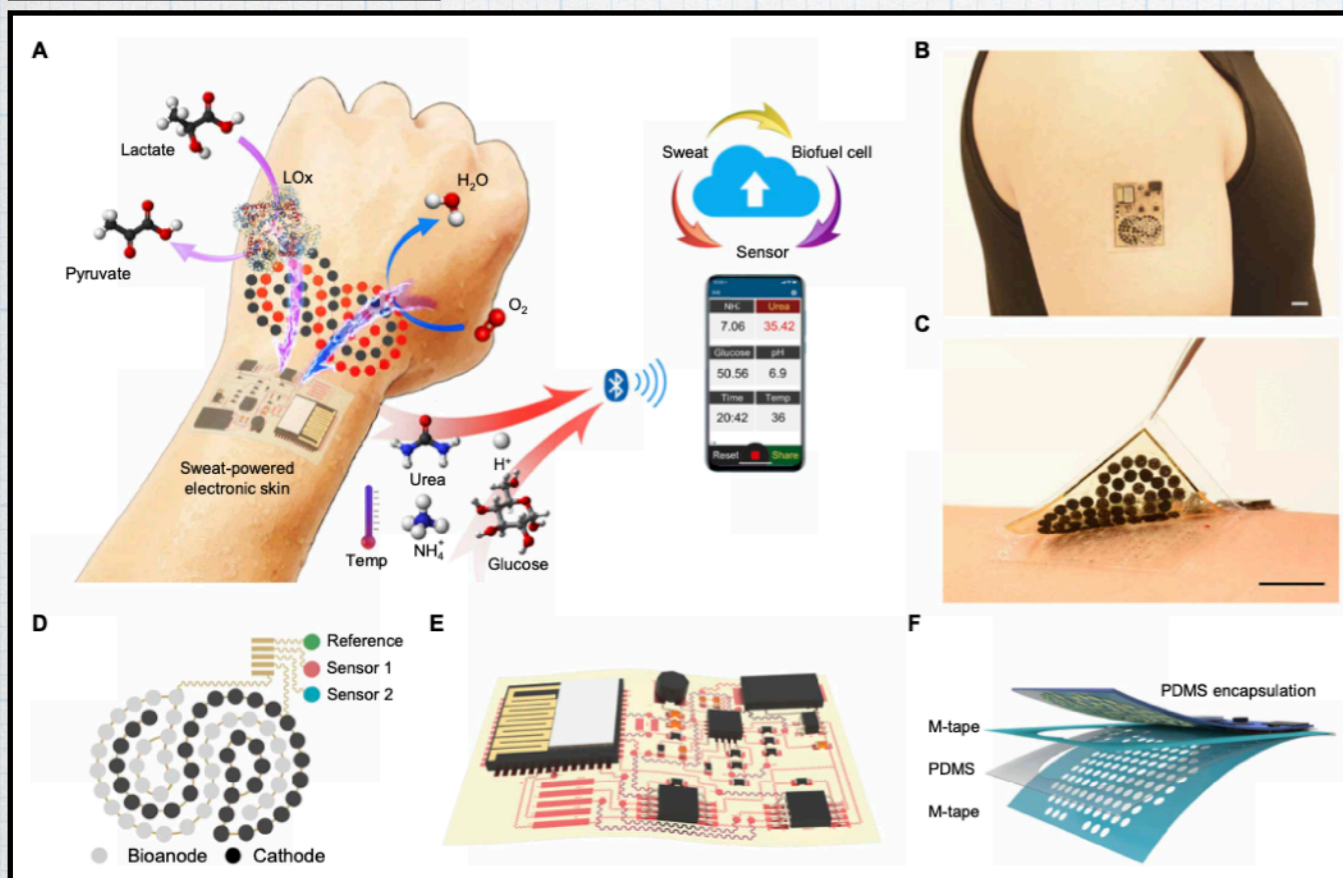
$$CD = \frac{I_{LH} - I_{RH}}{I_{LH} + I_{RH}}$$



Wearable technology: flexible transparent electronic device



- Electronic skins
- human-machine interfaces
- Soft robotics
- Health monitoring
- entertainment technology
- Harvesting solar energy

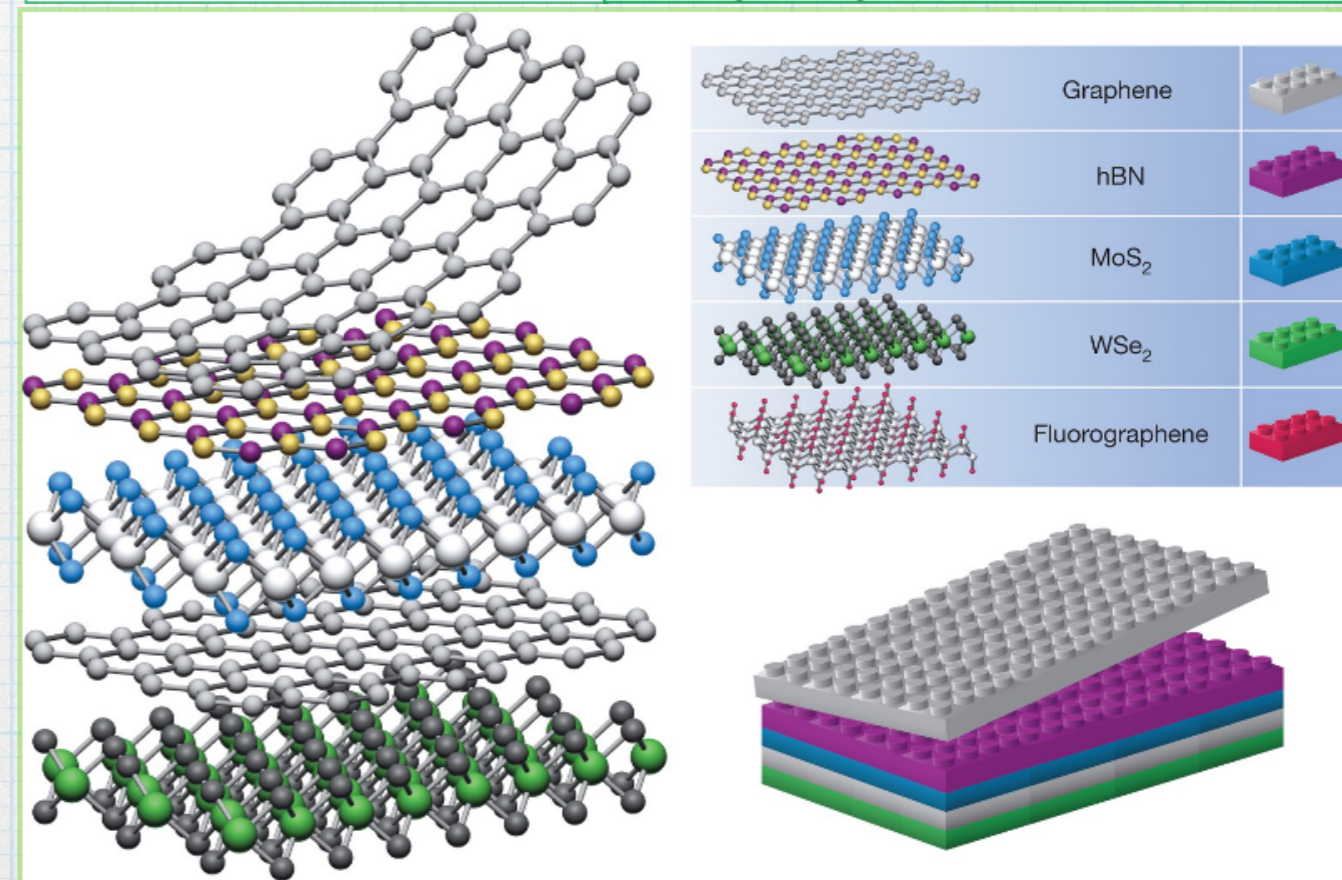
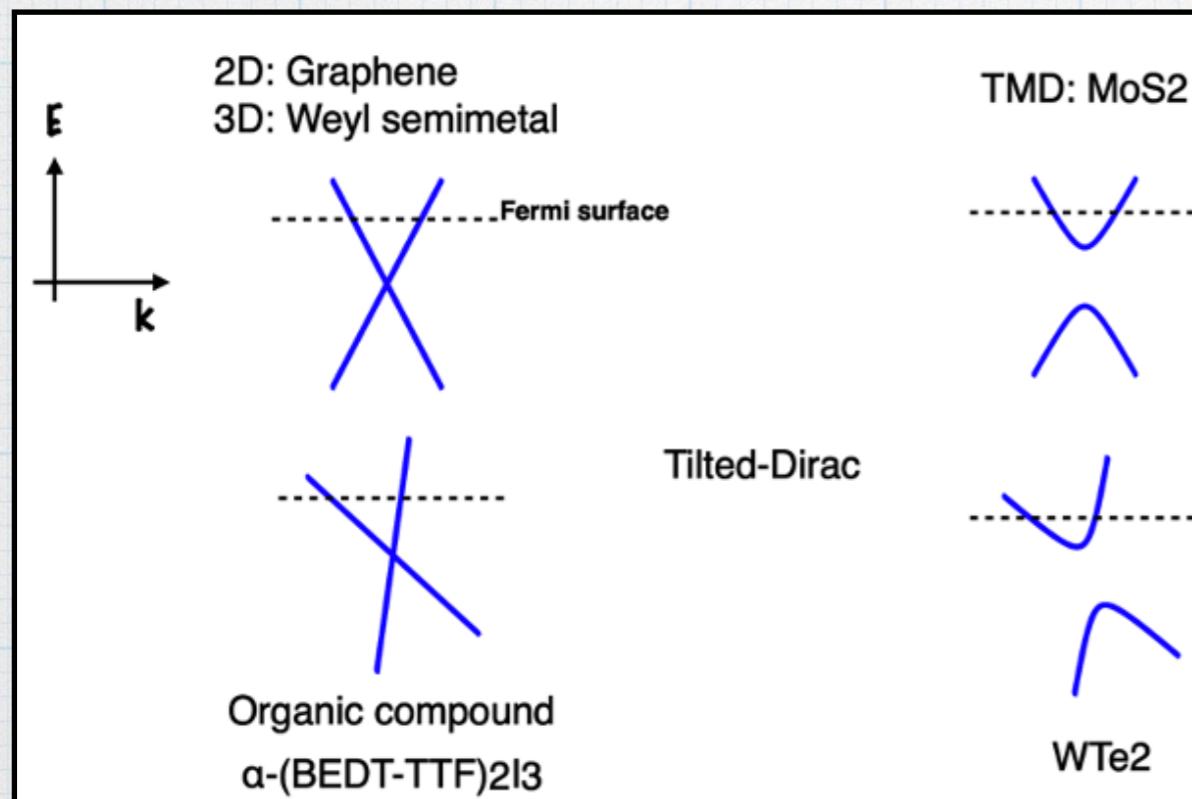
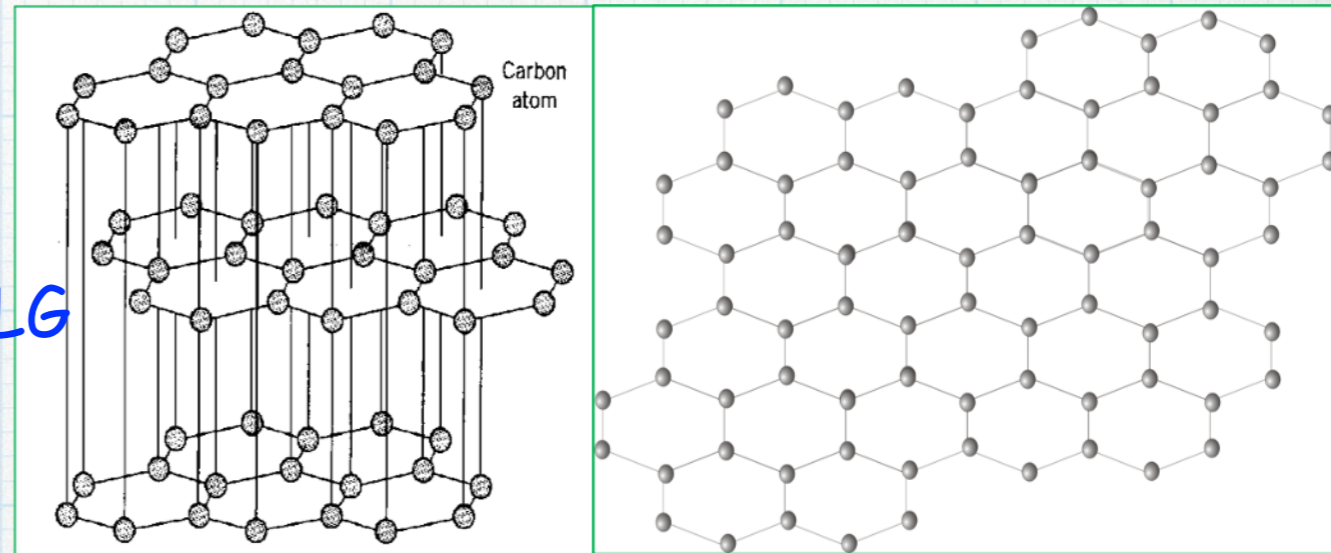


Yu et al., *Sci. Robot.* 5, eaaz7946 (2020)

Nature Electronics 3, 711 (2020)

Van der Waals Layered Materials

- Easy to incorporate in nanotechnology,
- Extraordinary mechanical properties: $\gamma \sim 1 \text{ TPA}$
- Universal properties: Dirac materials,
- High performance transport,
- Exotic optical properties,
- Strong many-body correlation: Twisted BLG
- Nontrivial topology: QSH in WTe_2



Nature 499, 419 (2013)

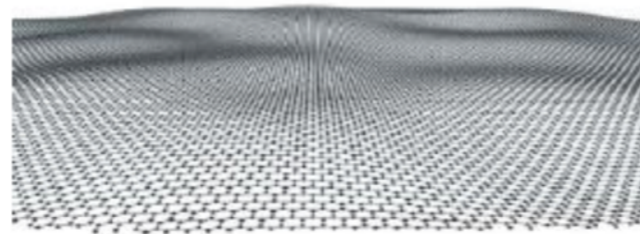
LETTERS

The structure of suspended graphene sheets

Jannik C. Meyer¹, A. K. Geim², M. I. Katsnelson³, K. S. Novoselov², T. J. Booth² & S. Roth¹



Scale bar, 500 nm



Ripple in Graphene

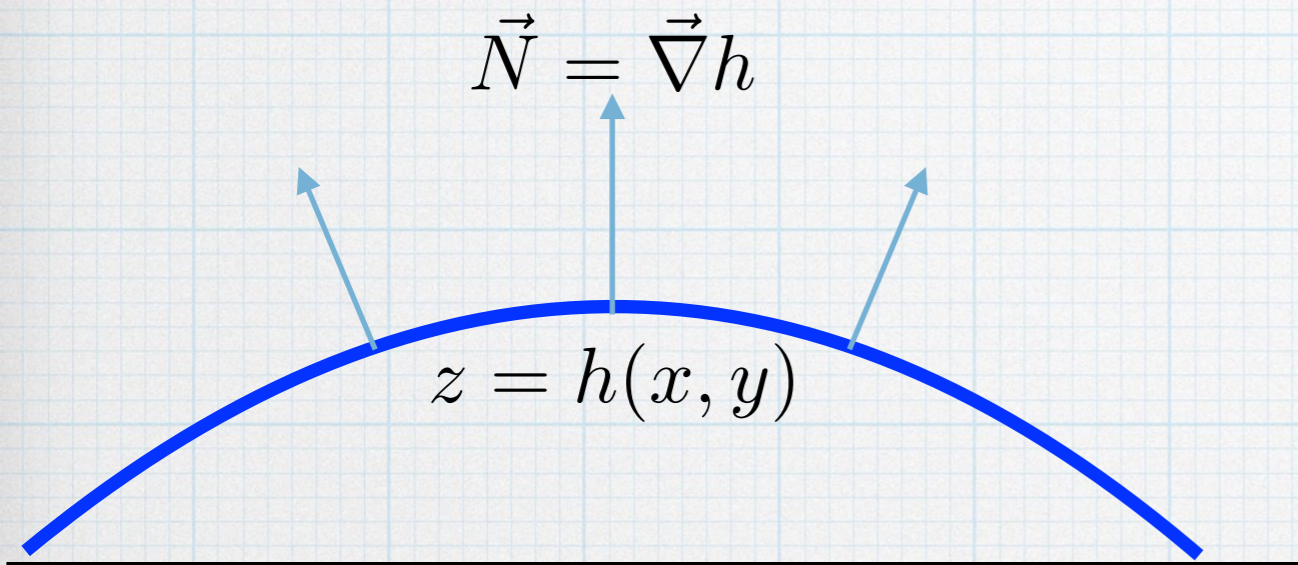
Measurement of the Elastic Properties and Intrinsic Strength of Monolayer Graphene

Changgu Lee,^{1,2} Xiaoding Wei,¹ Jeffrey W. Kysar,^{1,3} James Hone^{1,2,4*}

We measured the elastic properties and intrinsic breaking strength of free-standing monolayer graphene membranes by nanoindentation in an atomic force microscope. The force-displacement behavior is interpreted within a framework of nonlinear elastic stress-strain response, and yields second- and third-order elastic stiffnesses of 340 newtons per meter (N m^{-1}) and -690 N m^{-1} , respectively. The breaking strength is 42 N m^{-1} and represents the intrinsic strength of a defect-free sheet. **These quantities correspond to a Young's modulus of $E = 1.0$ terapascals, third-order elastic stiffness of $D = -2.0$ terapascals, and intrinsic strength of $\sigma_{\text{int}} = 130$ gigapascals for bulk graphite. These experiments establish graphene as the strongest material ever measured,** and show that atomically perfect nanoscale materials can be mechanically tested to deformations well beyond the linear regime.

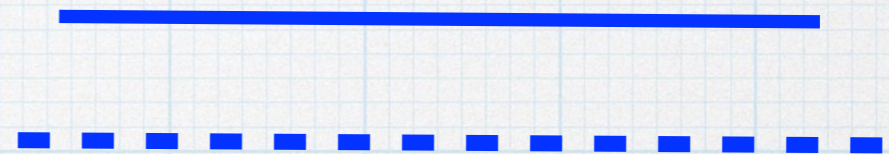
Graphene as a 2D elastic membrane

Bending energy



$$F_b \approx \frac{1}{2} \kappa \int dx dy (\vec{\nabla} \cdot \vec{N})^2$$
$$= \frac{1}{2} \kappa \int dx dy (\nabla^2 h)^2$$

Stretching energy



$$F_t \approx Y \int dx dy \{ \sqrt{1 + |\nabla h|^2} - 1 \}$$
$$\approx \frac{1}{2} Y \int dx dy |\nabla h|^2$$

1 TPa

0.1 nm

$$Y_{2D} = Y_{3D} t \sim 10^{12} \text{N/m}^2 \times 10^{-10} \text{m} \sim 100 \text{N/m}$$

Föppl-von Kármán number νK

$$\nu K = \frac{Y_{2D} L^2}{\kappa} \quad \kappa \sim Y_{2D} t^2 / 10$$

Y_{2D} : two-dimensional Young's modulus ($[Y_{2D}] = \text{N/m}$)

κ : bending rigidity ($[\kappa] = \text{J}$)

L : sheet side length

t : sheet thickness

$$\nu K \sim 10 (L/t)^2$$

$$L \sim 100 \text{ nm},$$

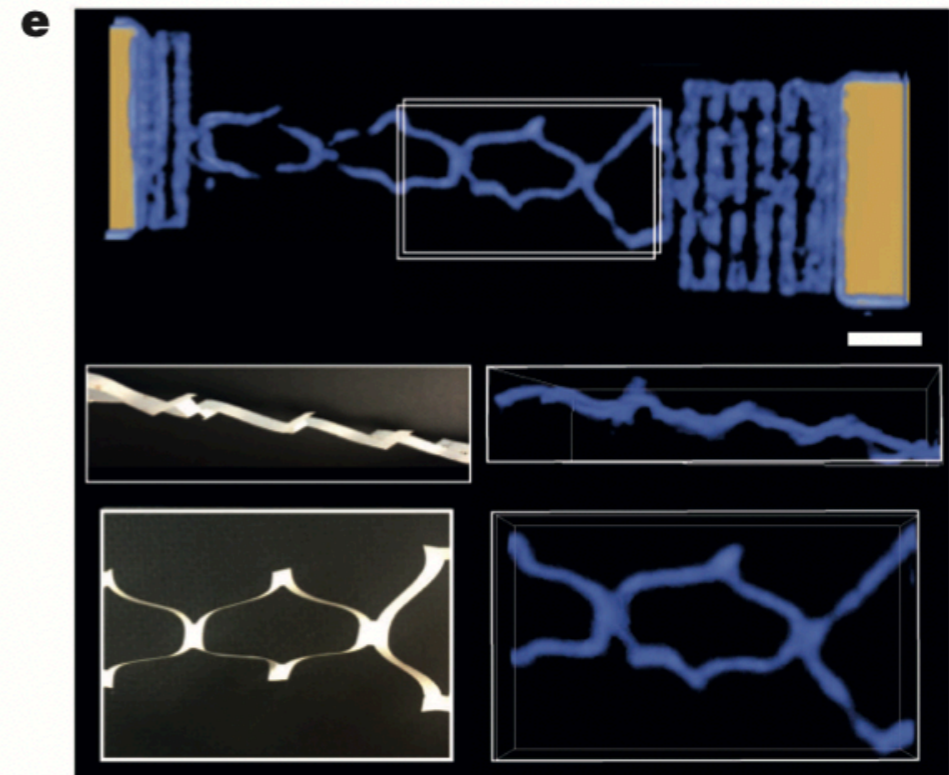
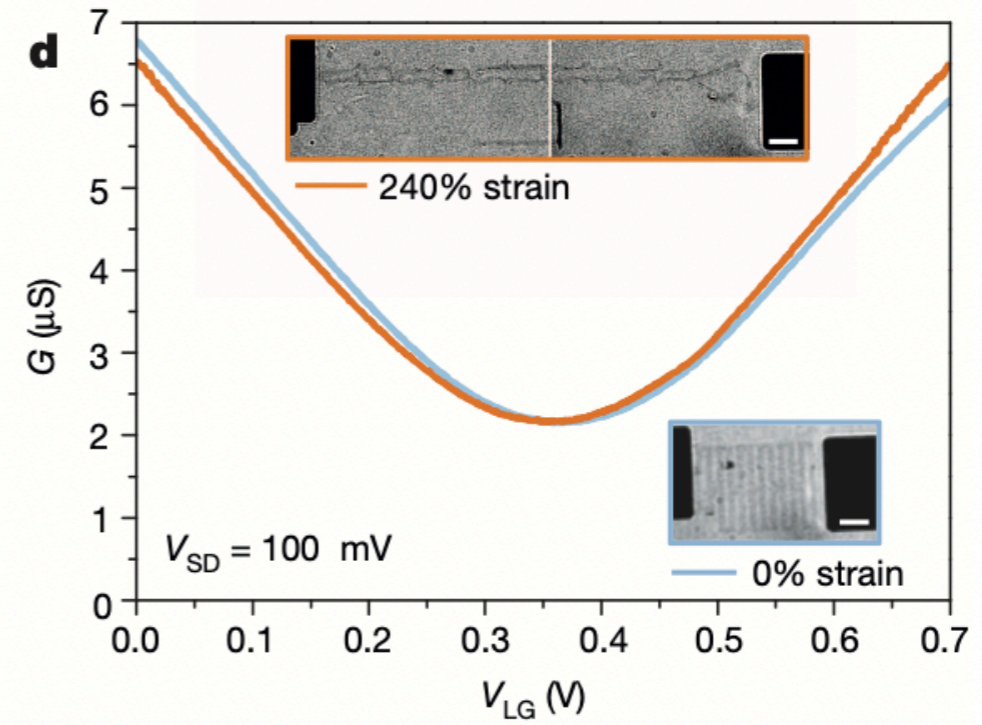
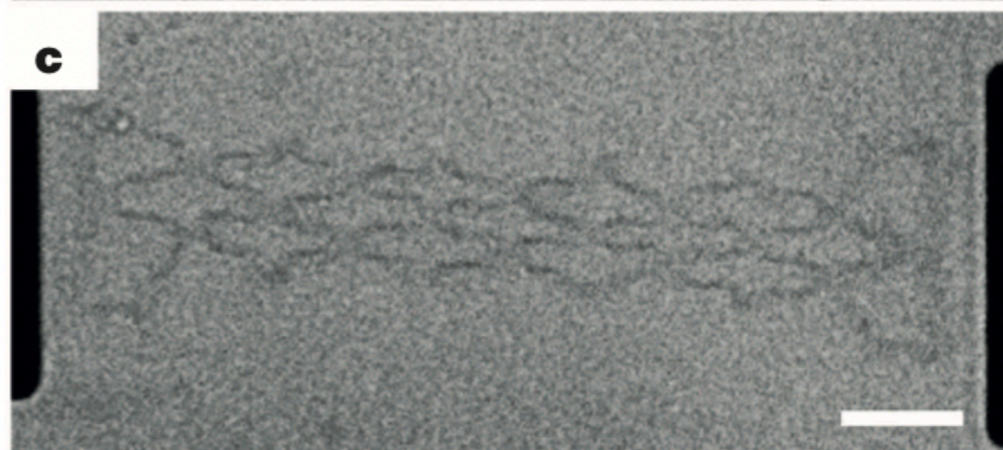
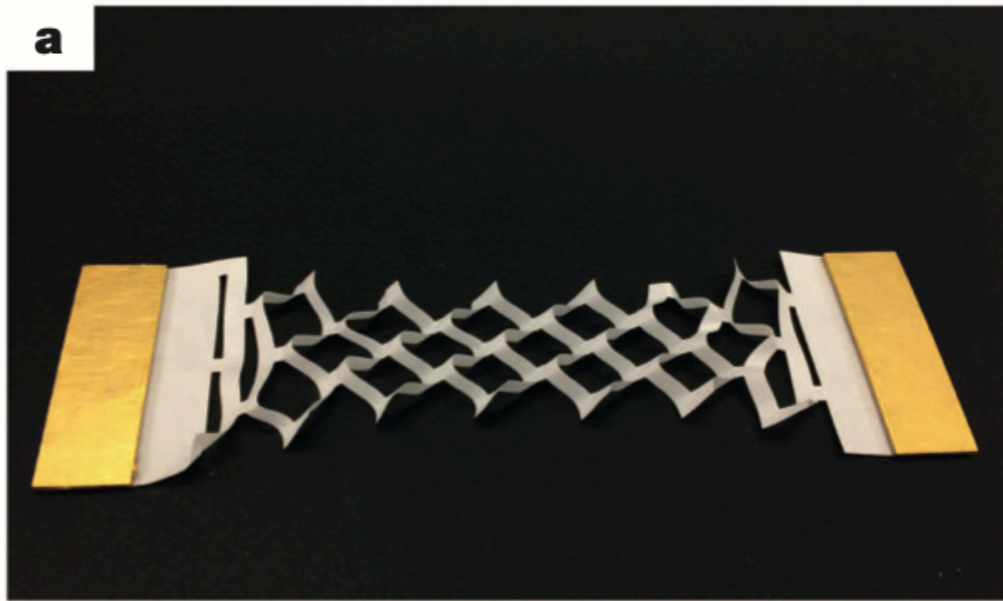
$$\text{paper: } t \sim 0.1 \text{ mm} \rightarrow \nu K \sim 10^{-5}$$

$$\text{graphene: } t \sim 0.1 \text{ nm} \rightarrow \nu K \sim 10^7$$

For large νK we can easily bend the sheet without energy cost for stretching.

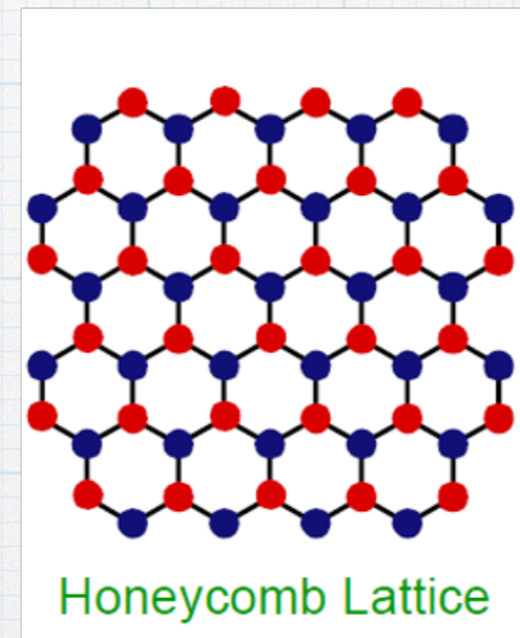
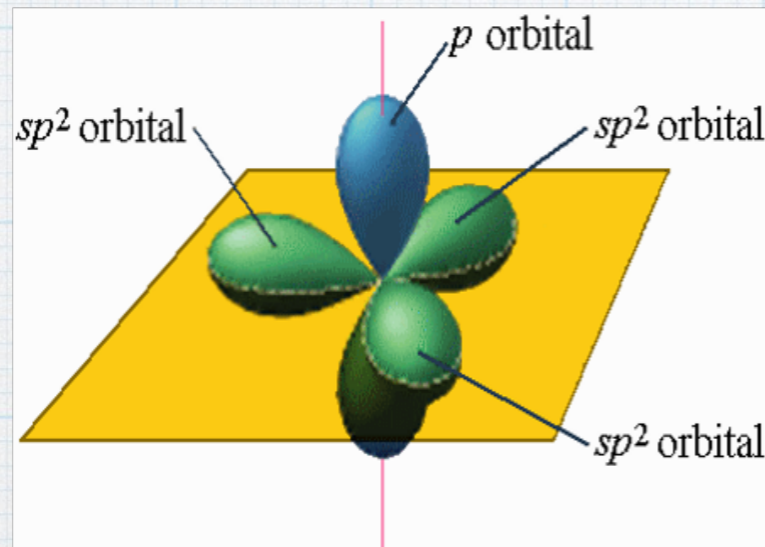
Graphene kirigami

Nature 524, 204–207 (2015)

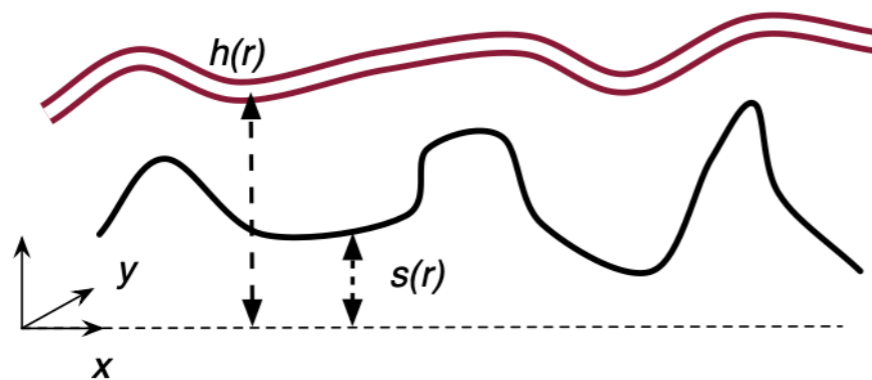


Graphene as an electronic membrane

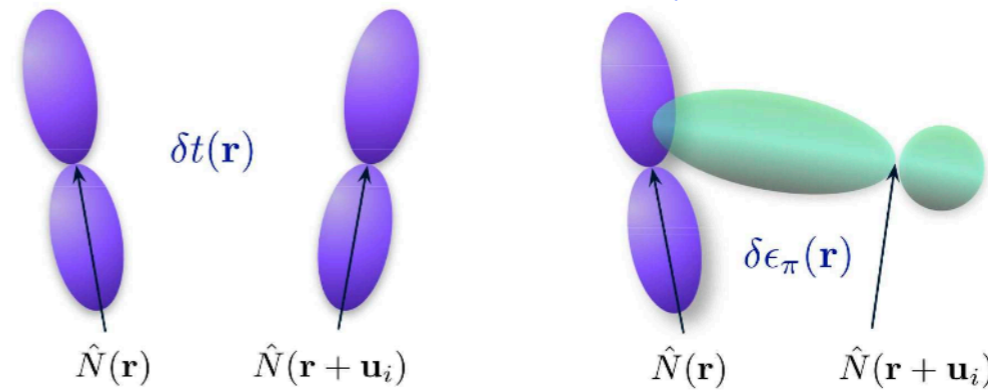
Carbon atom : $1s^2 2s^2 2p^2$
 : *(two)* $1s^2$ + *(three)* sp^2 + *(one)* $2p_z$



How curvature and strain can affect electronic structure of graphene?



(a)



(b)

(c)

Euophysics Letters 84, 57007 (2008)

Flexible and transparent devices



Extraordinary
Young's Modulus $\sim 1\text{TPa}$

Highly flexible to
out-of-plane deformation

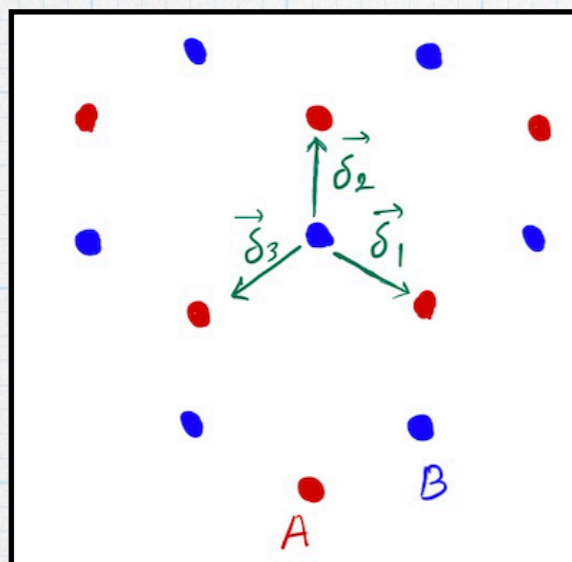
Ab initio: not practical for inhomogeneous strain

Curve space field theory: missing crystal symmetry

Tight-binding theory

K.p (invariant) method

Pseudo gauge field in hexagonal lattice



$$H = \sum_{R, \delta} t_{\delta} a_R^{\dagger} b_{R+\delta} + \text{c.c.}$$

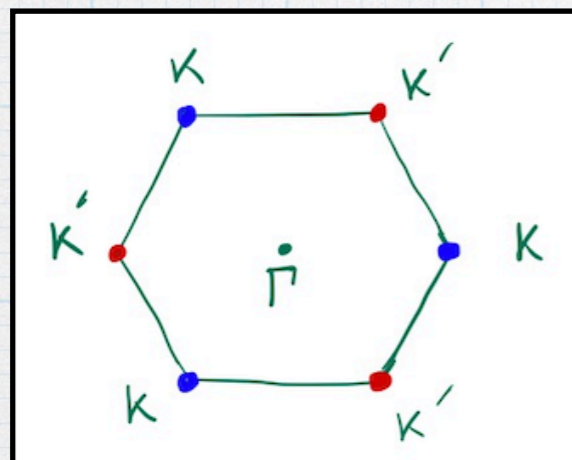
$$a_R = \frac{1}{\sqrt{N}} \sum_{\mathbf{k}} e^{i\mathbf{k} \cdot \mathbf{R}} a_{\mathbf{k}}$$

$$b_R = \frac{1}{\sqrt{N}} \sum_{\mathbf{k}} e^{i\mathbf{k} \cdot \mathbf{R}} b_{\mathbf{k}}$$

$$H = \sum_{\mathbf{k}} (a_{\mathbf{k}}^{\dagger} \ b_{\mathbf{k}}) \hat{H}_{\mathbf{k}} \begin{pmatrix} a_{\mathbf{k}} \\ b_{\mathbf{k}} \end{pmatrix}$$

$$\hat{H}_{\mathbf{k}} = \begin{pmatrix} 0 & f_{\mathbf{k}} \\ f_{\mathbf{k}}^* & 0 \end{pmatrix}$$

$$f_{\mathbf{k}} = \sum_{\delta} t_{\delta} e^{-i\mathbf{k} \cdot \delta}$$



No strain: $t_{\delta} = t_0$ $\xrightarrow[\vec{k} = \vec{K} + \mathbf{q}]{q \ll K}$ $f_{\mathbf{q}} \sim t_0 (q_x - i q_y)$

$$\hat{H} \sim \vec{\sigma} \cdot \vec{q}$$

Dirac model

$$\hat{\sigma}_x = \tau \begin{pmatrix} 0 & 1 \\ 1 & 0 \end{pmatrix}, \quad \hat{\sigma}_y = \begin{pmatrix} 0 & -i \\ i & 0 \end{pmatrix}$$

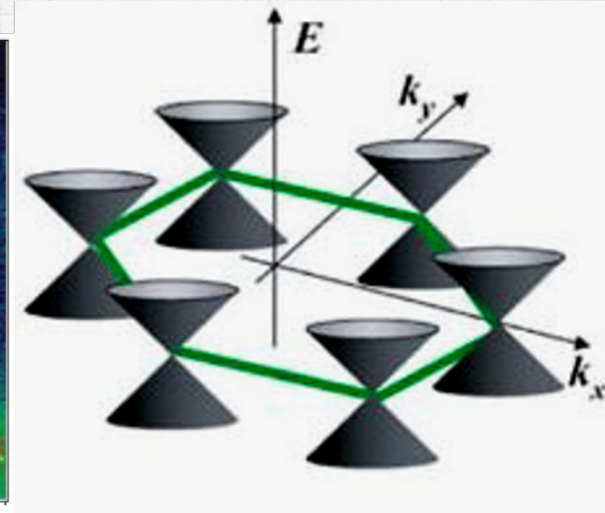
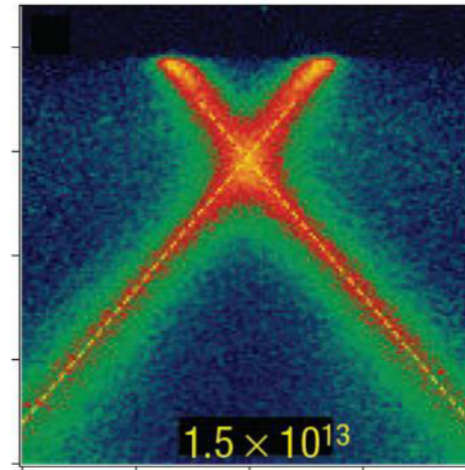
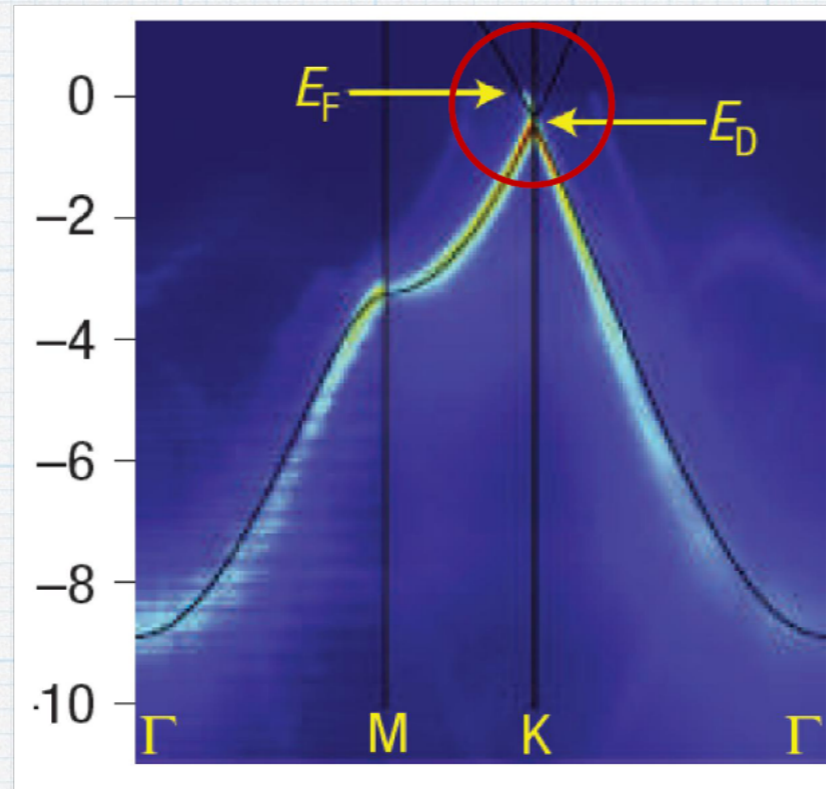
$$\hat{H} \sim \vec{\sigma} \cdot (\vec{q} + \tau e \vec{A})$$

pseudo gauge field:

$$A_x = t_{\delta_2} - \frac{t_{\delta_1} + t_{\delta_3}}{2}, \quad A_y = \frac{\sqrt{3}}{2} (t_{\delta_1} - t_{\delta_3})$$

$\tau = +1 \longrightarrow K$ valley
 $\tau = -1 \longrightarrow K'$ valley

Angle-resolved photoelectron spectroscopy (ARPES)



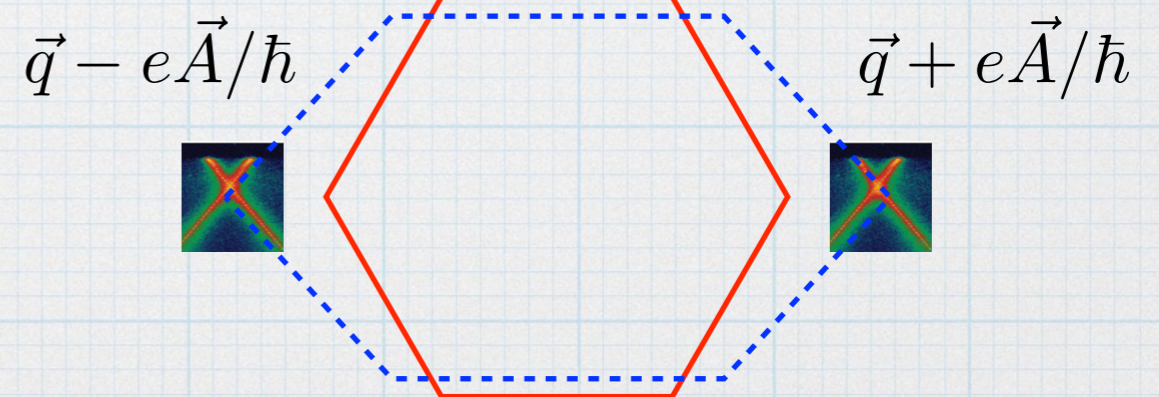
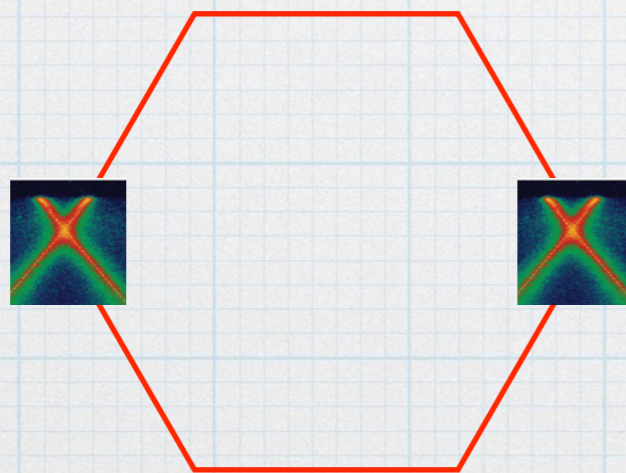
$$\mathcal{H} = \hbar v_F (\tau q_x \sigma_x + q_y \sigma_y)$$

$$v_F = \frac{3ta_0}{2\hbar} \approx 10^6 \frac{m}{s} \approx \frac{c}{300}$$

Each state is 4-fold degenerate, 2 for spin and 2 for valley

A. Bostwick, et al, 2007, Nature Physics 3(1), 36.

Uniaxial strain



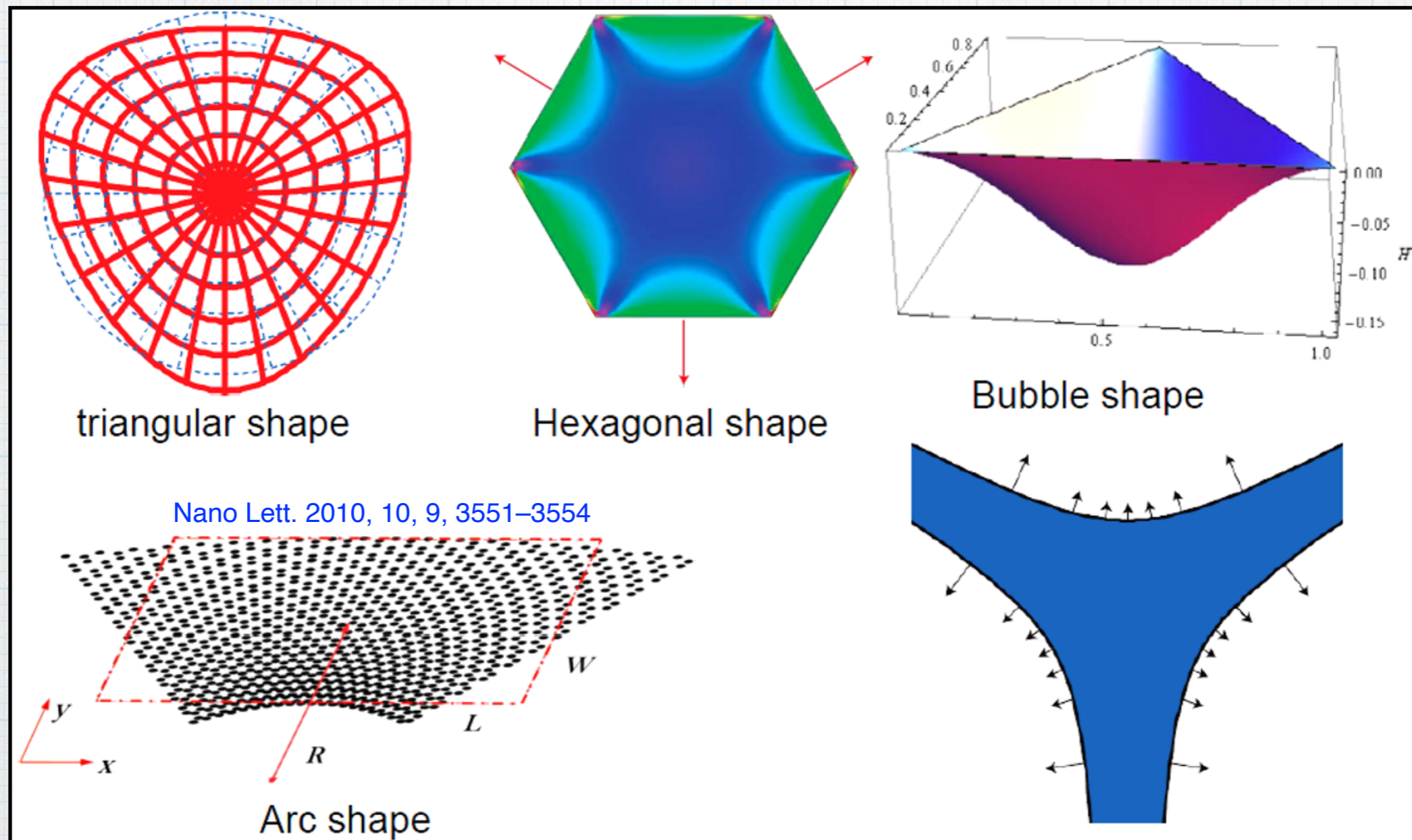
Uniform pseudomagnetic field

$$A_x = \beta(\hbar/ea)(u_{xx} - u_{yy})$$

$$A_y = \beta(\hbar/ea)(-2u_{xy})$$

$$\vec{B} = \vec{\nabla} \times \vec{A}$$

$$\beta = -\frac{\partial \ln t}{\partial \ln a}$$

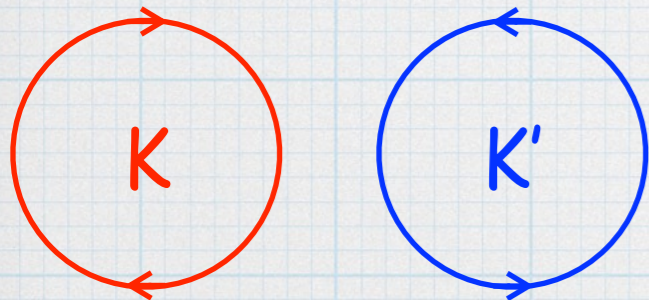
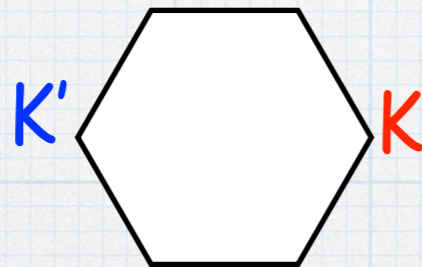
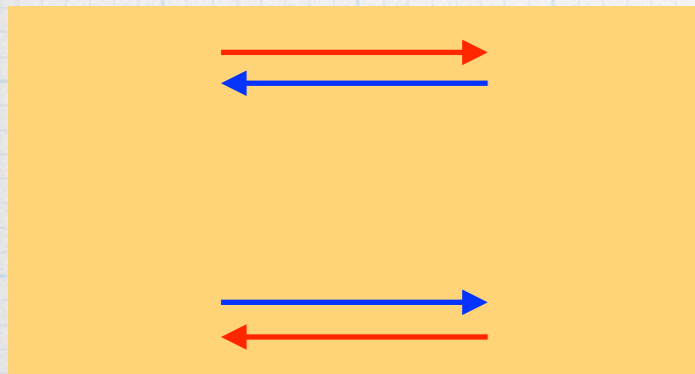
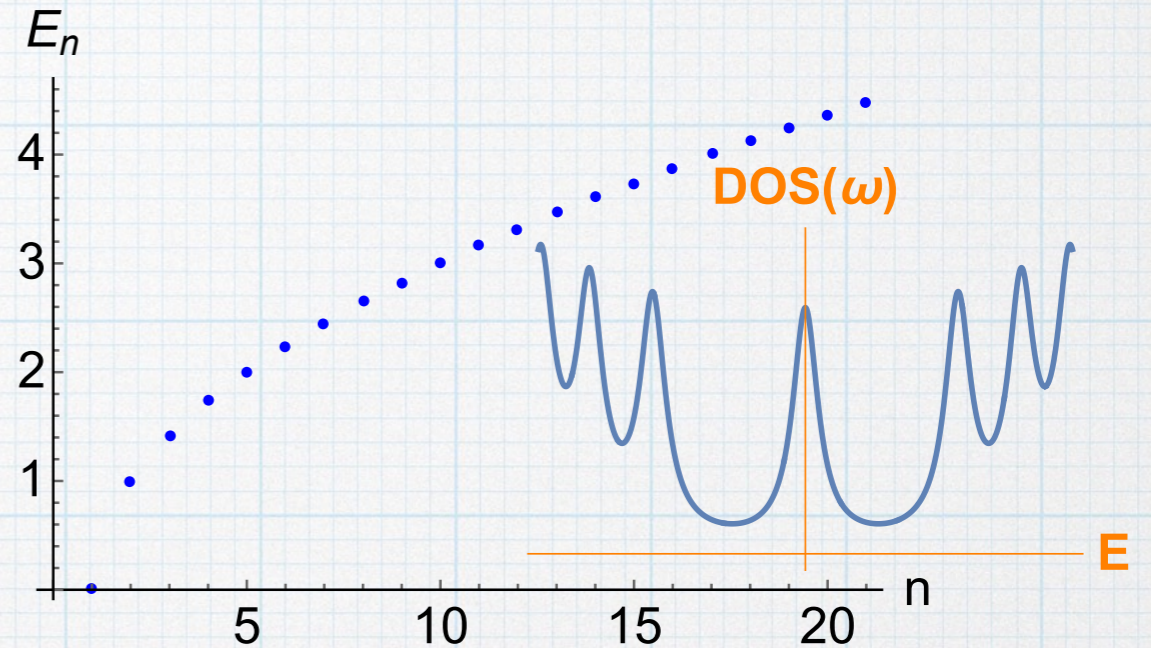


Guinea, F., Katsnelson, M. & Geim, A. Nature Phys 6, 30-33 (2010)

LDOS: Pseudo Landau Levels

$$H = v_F \hat{\sigma} \cdot (\mathbf{p} + e\mathbf{A}) \quad \mathbf{B} = \nabla \times \mathbf{A}$$

$$E_n \approx 35\text{meV} \times \text{sign}(n) \times \sqrt{B[T]} \times \sqrt{|n|}$$



Quantum valley Hall effect

LETTERS
PUBLISHED ONLINE: 27 SEPTEMBER 2009 | DOI: 10.1038/NPHYS1420

nature
physics

Energy gaps and a zero-field quantum Hall effect in graphene by strain engineering

F. Guinea^{1*}, M. I. Katsnelson² and A. K. Geim^{3*}

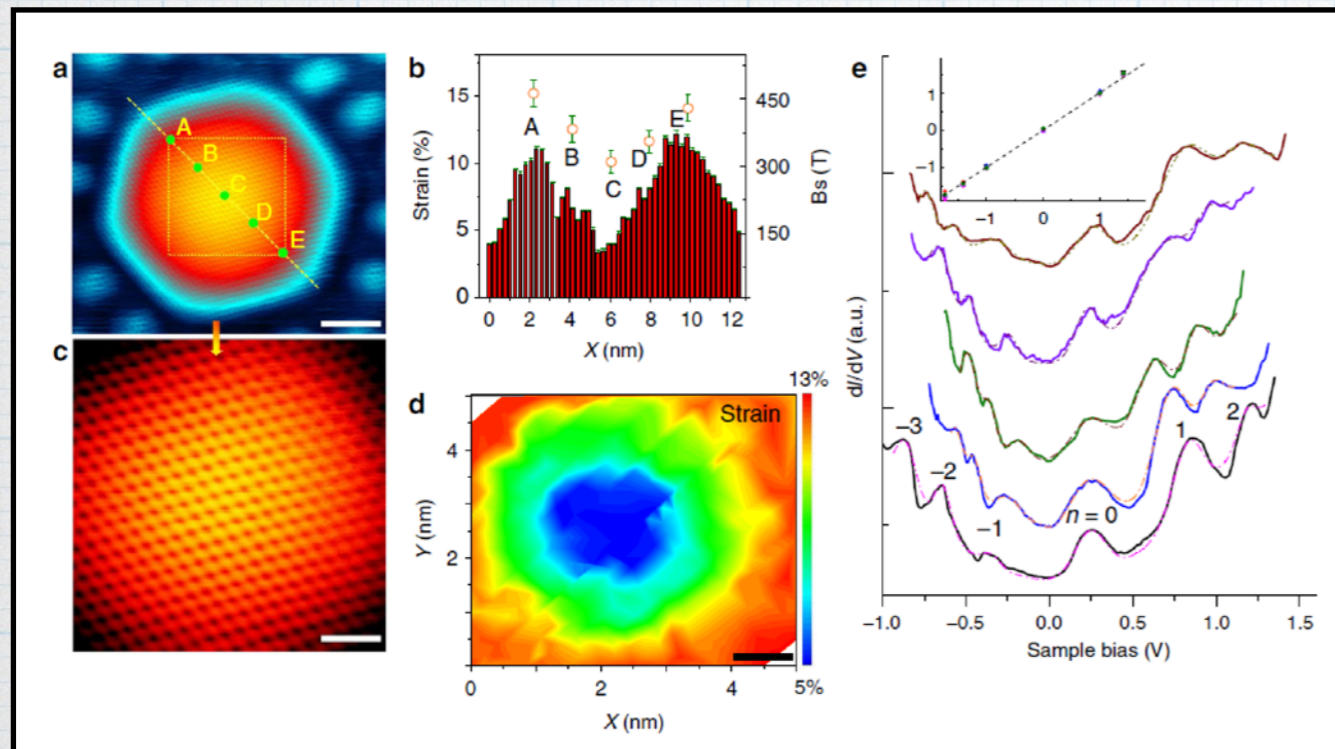
Science
AAAS

Strain-Induced Pseudo-Magnetic Fields Greater Than 300 Tesla in Graphene Nanobubbles
N. Levy, *et al.*
Science **329**, 544 (2010);
DOI: 10.1126/science.1191700

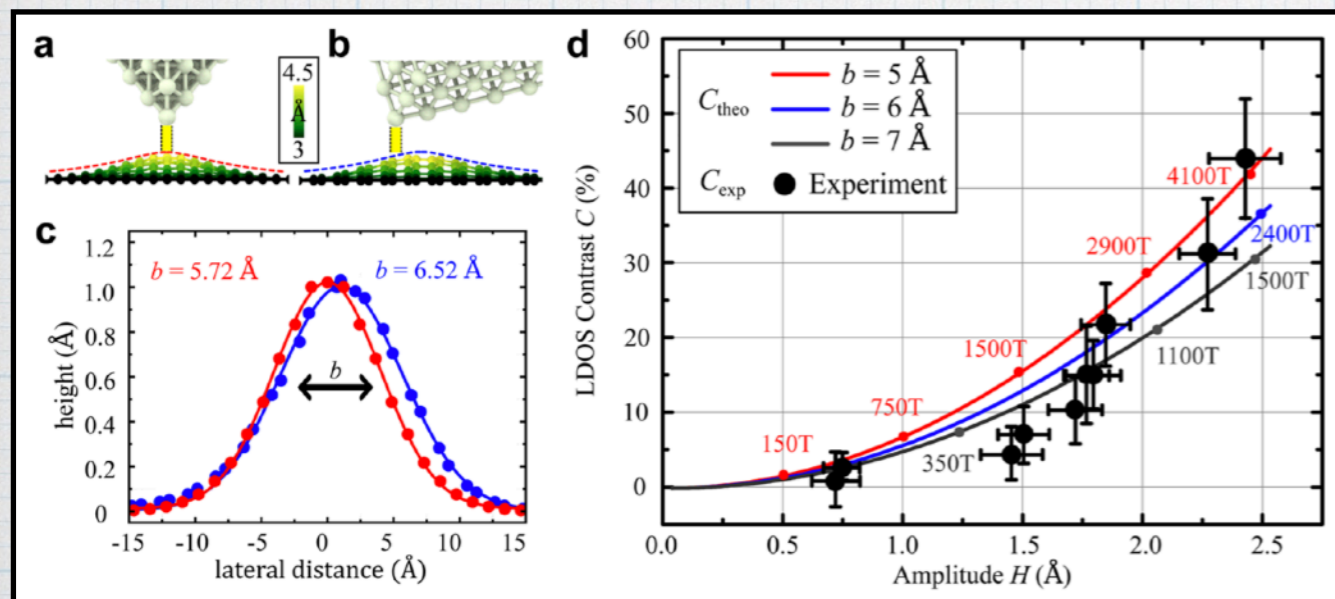
B

A

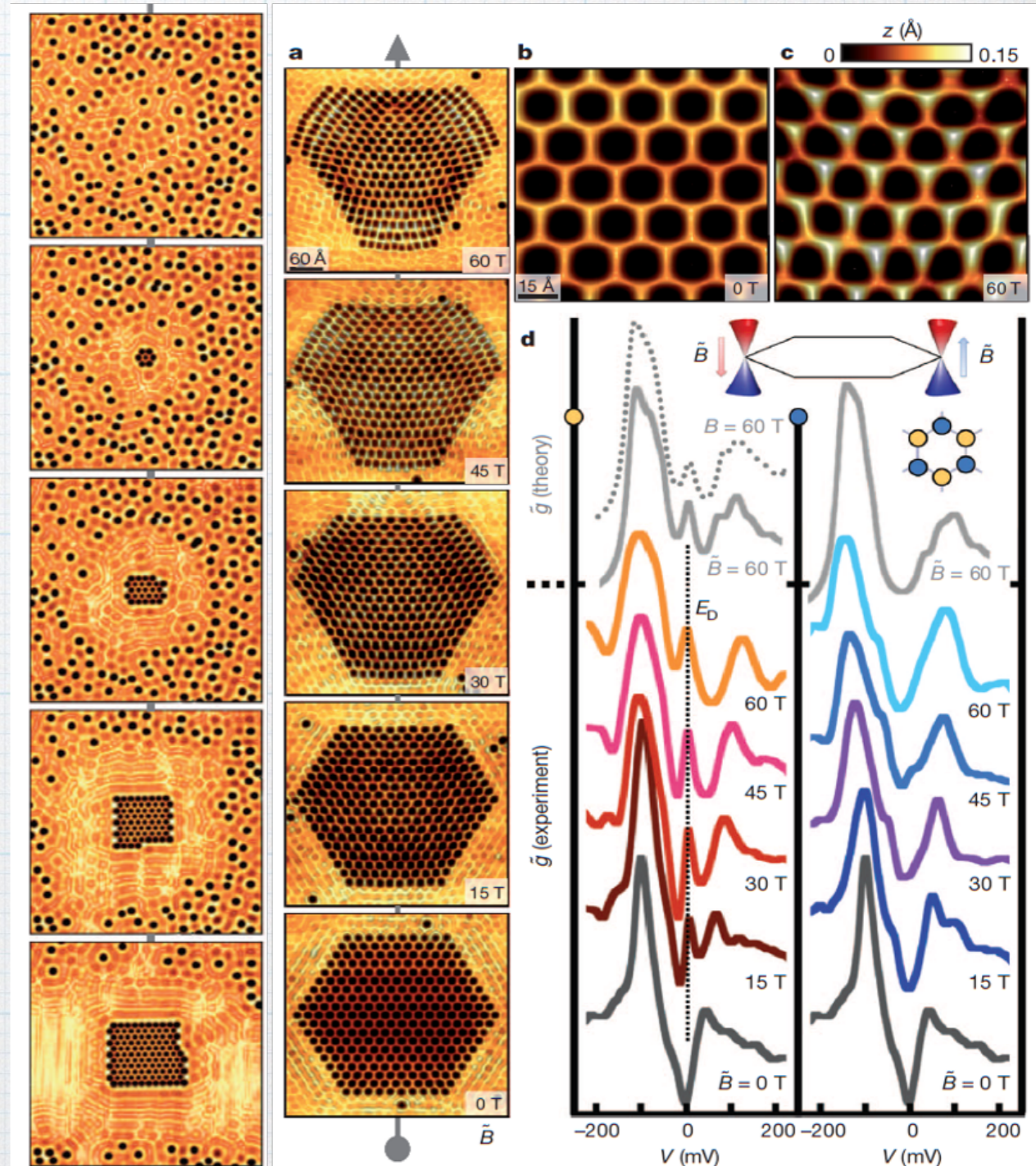
Pseudo Landau Levels



Nat Commun 3, 823 (2012)



Nano Lett. 2017, 17, 2240–2245



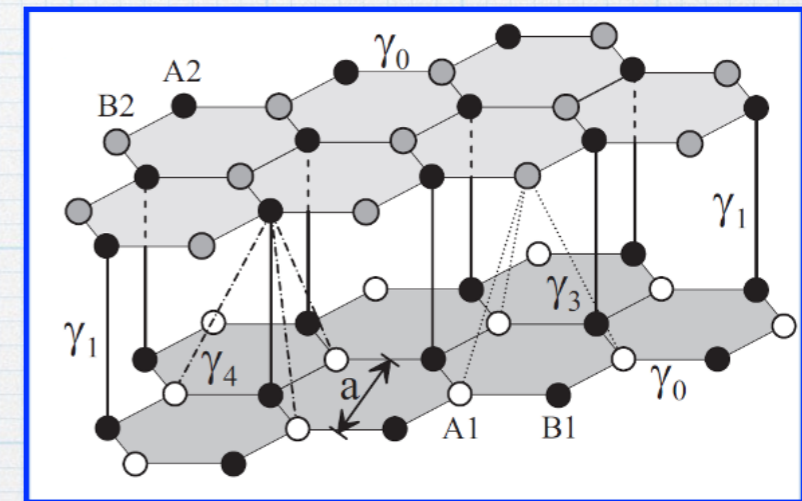
K. K. Gomes, et. al , Nature,483 306 (2012)

Starined BLG: Tight-binding Hamiltonian

$$\begin{aligned}
 H = & \sum_{i,l} \{ \epsilon_i^a a_i^{l\dagger} a_i^l + \epsilon_i^b b_i^{l\dagger} b_i^l \} \\
 & - \sum_{\langle ij \rangle, l} \{ \gamma_0^{ij} e^{\phi_{ij}} a_i^{l\dagger} b_j^l + H.c. \} \\
 & - \sum_i \{ \gamma_1^{ij} a_i^{2\dagger} b_i^1 + H.c. \} \\
 & - \sum_{\langle ij \rangle} \{ \gamma_3^{ij} e^{\phi_{ij}} a_i^{1\dagger} b_j^2 + H.c. \}
 \end{aligned}$$

$$\phi_{ij} = \frac{e}{\hbar} \int_i^j \vec{A} \cdot d\vec{r}$$

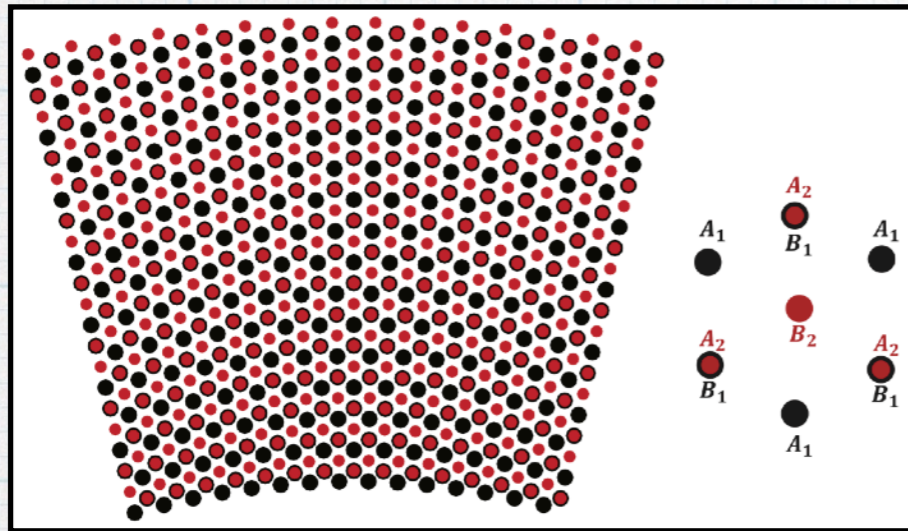
$$\epsilon_i = (-1)^l \frac{u}{2}$$



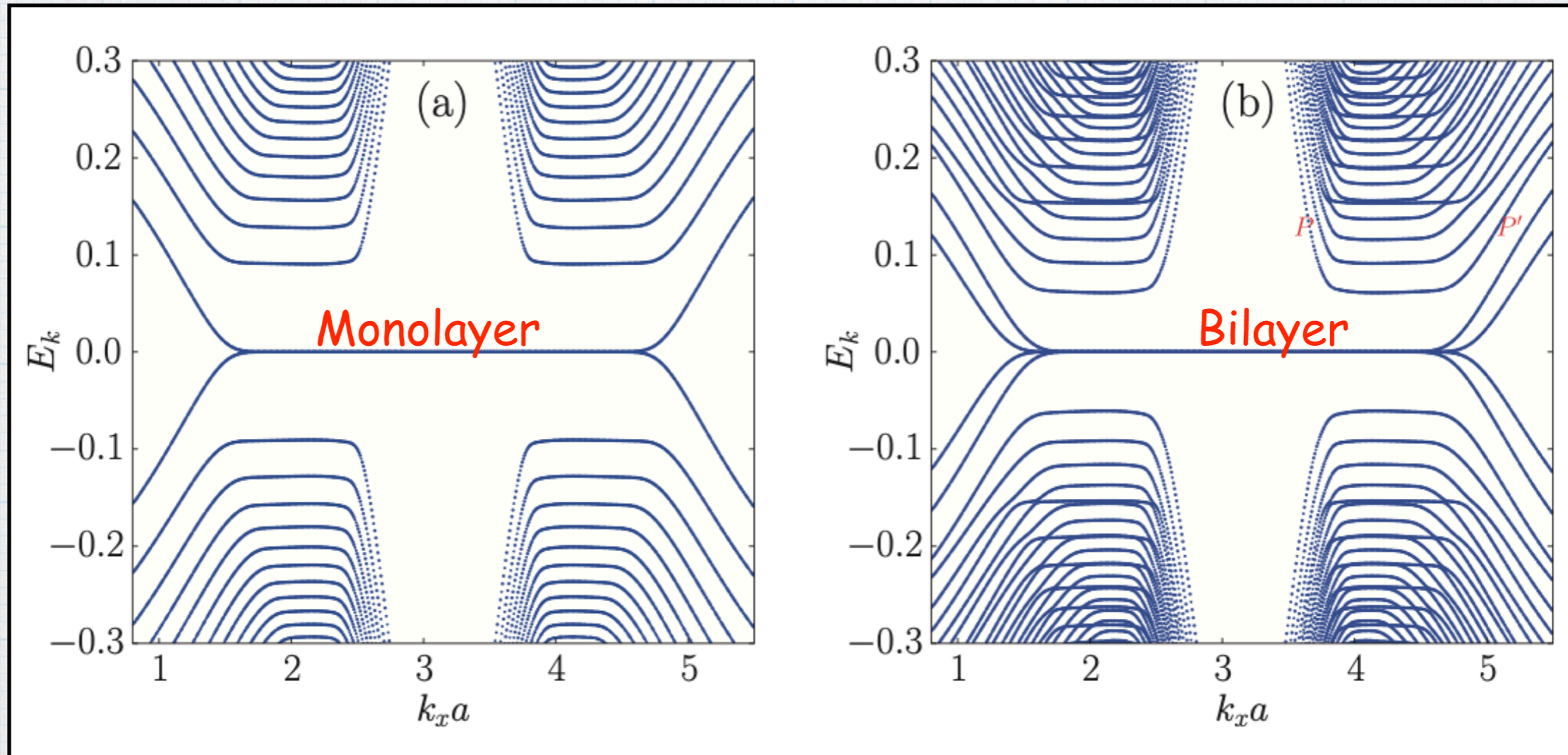
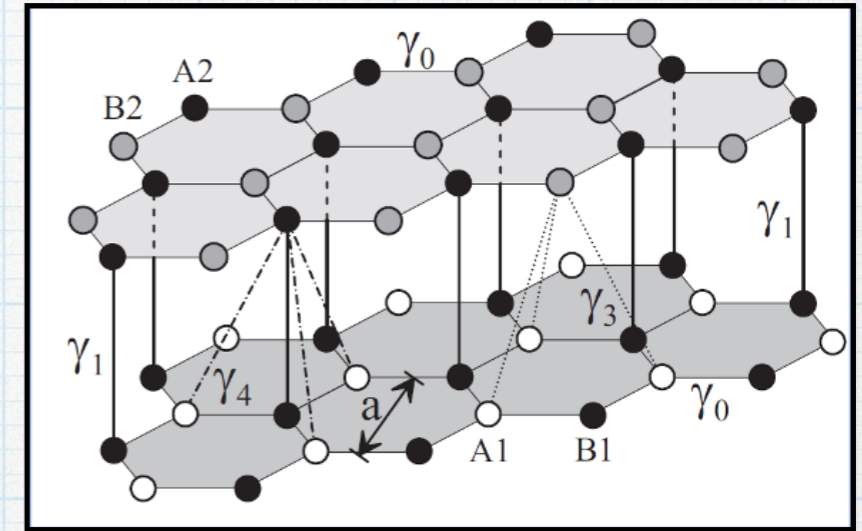
$$\gamma_0^{ij} = \gamma_0 e^{-\beta_0 \left(\frac{d}{a_0} - 1 \right)}, \quad \gamma_1^{ij} = \gamma_1 e^{-\beta_1 \left(\frac{d}{c_0} - 1 \right)}$$

$$\gamma_3^{ij} = X \left[\gamma_0 \left(\frac{d_{\parallel}}{d} \right)^2 e^{-\beta_0 \left(\frac{d}{\tilde{c}_0} - 1 \right)} + \gamma_1 \left(\frac{d_{\perp}}{d} \right)^2 e^{-\beta_1 \left(\frac{d}{\tilde{c}_0} - 1 \right)} \right]$$

PLL in arc-shaped Bilayer Graphene

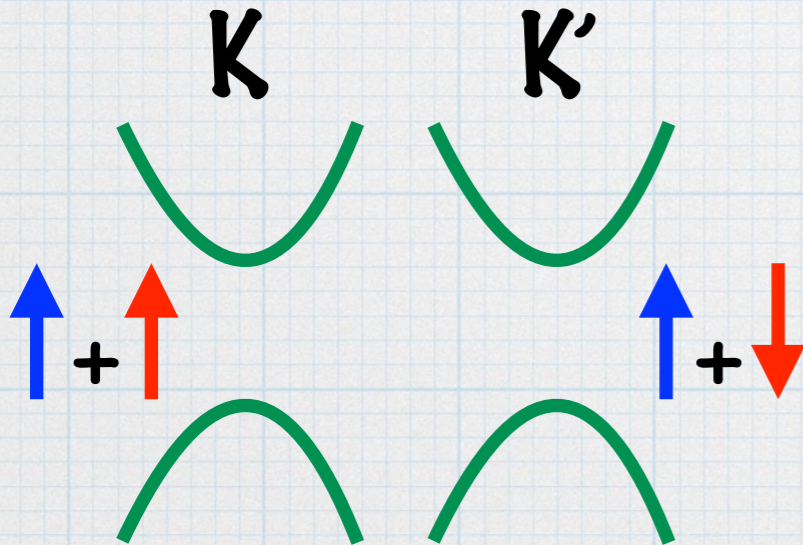
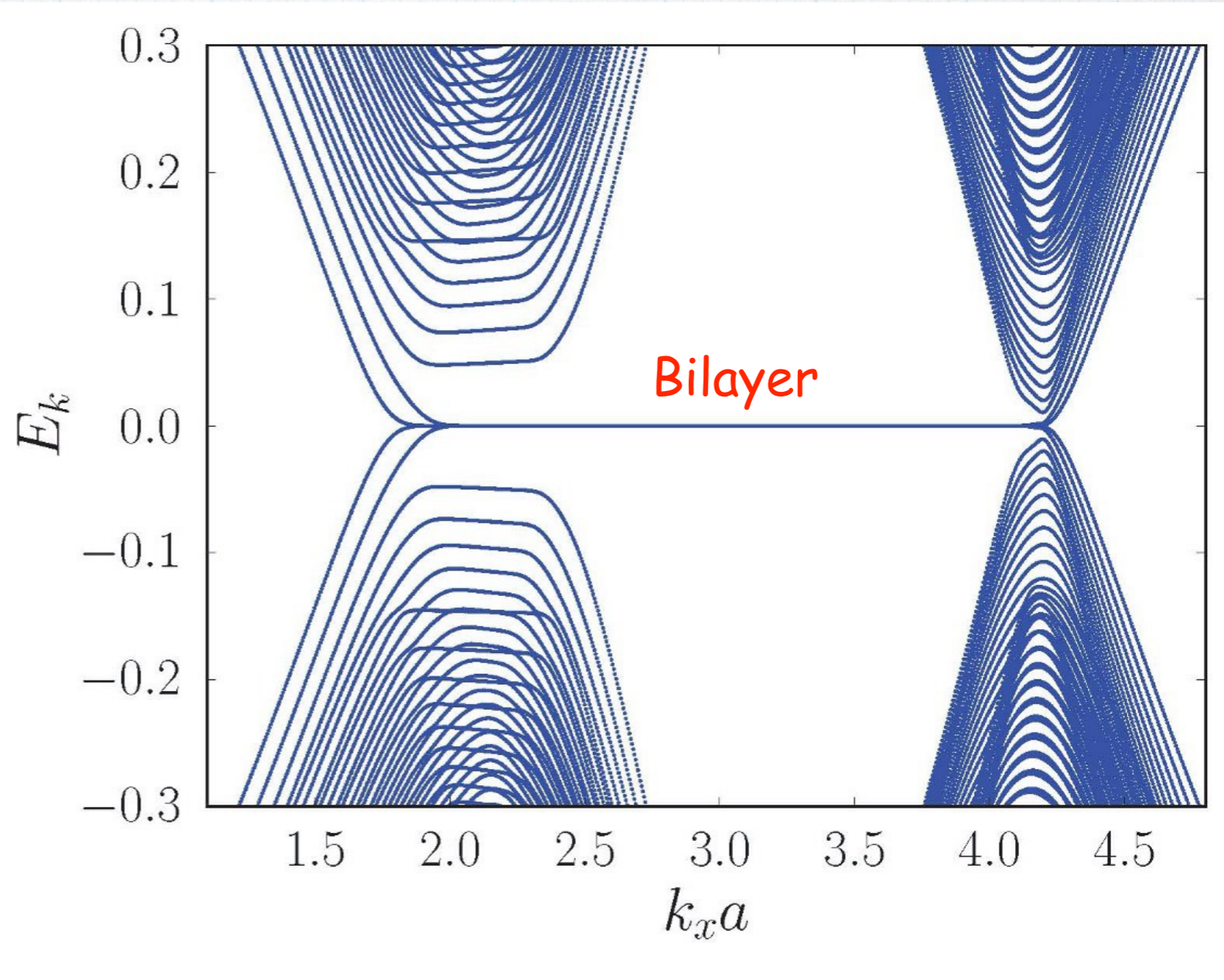
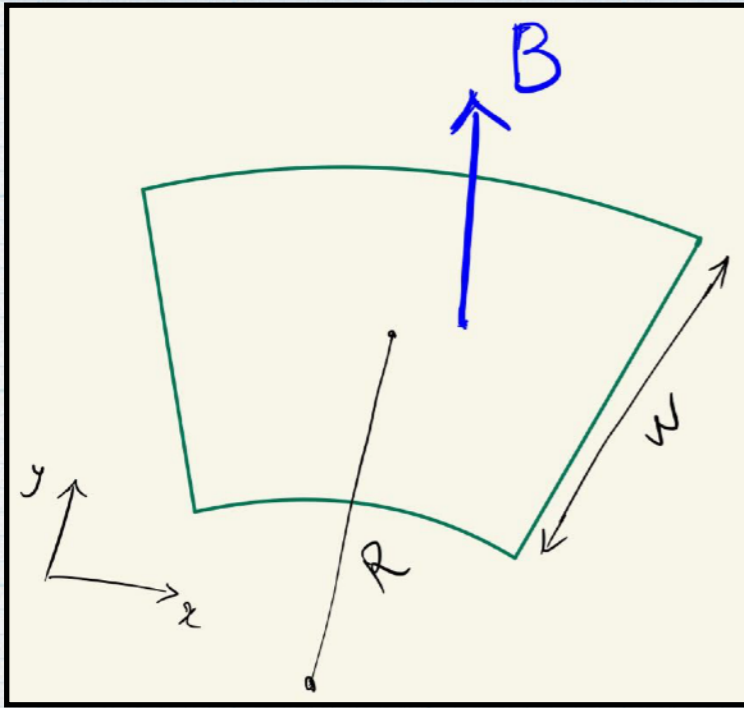


$$(u_x, u_y) = \left(\frac{xy}{R}, -\frac{x^2}{2R} \right)$$



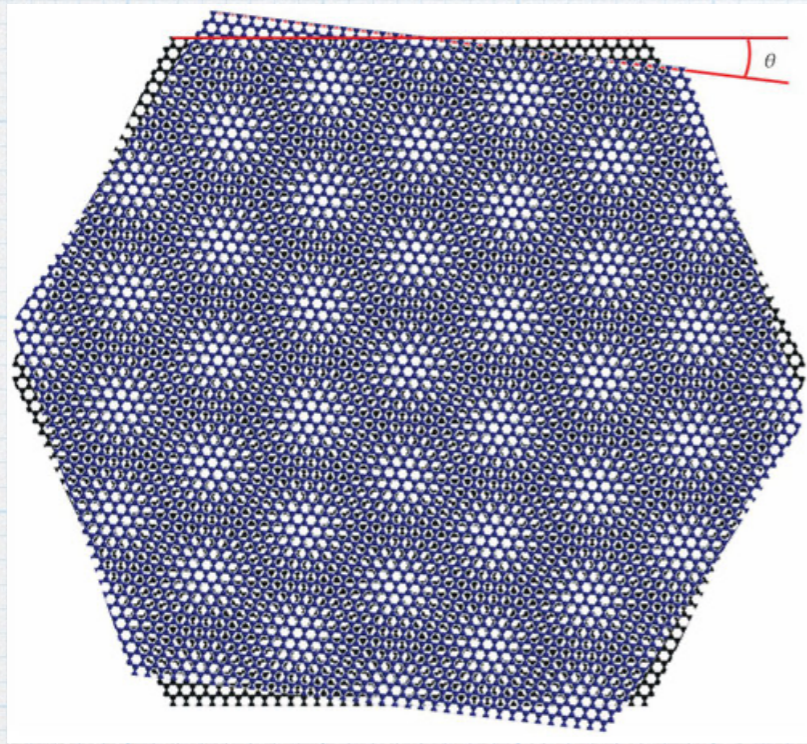
HR and Reza Asgari, Phys. Rev. B 88, 035404 (2013)

Real B + Pseudo B



HR and Reza Asgari, Phys. Rev. B 88, 035404 (2013)

Relative twist of layers



PNAS July 26, 2011 108 (30) 12233-12237

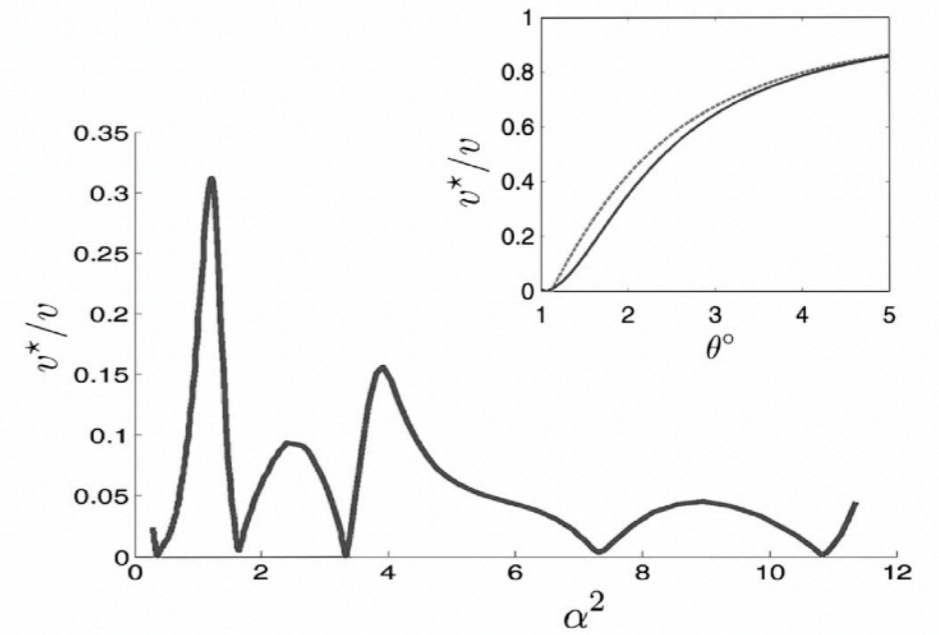
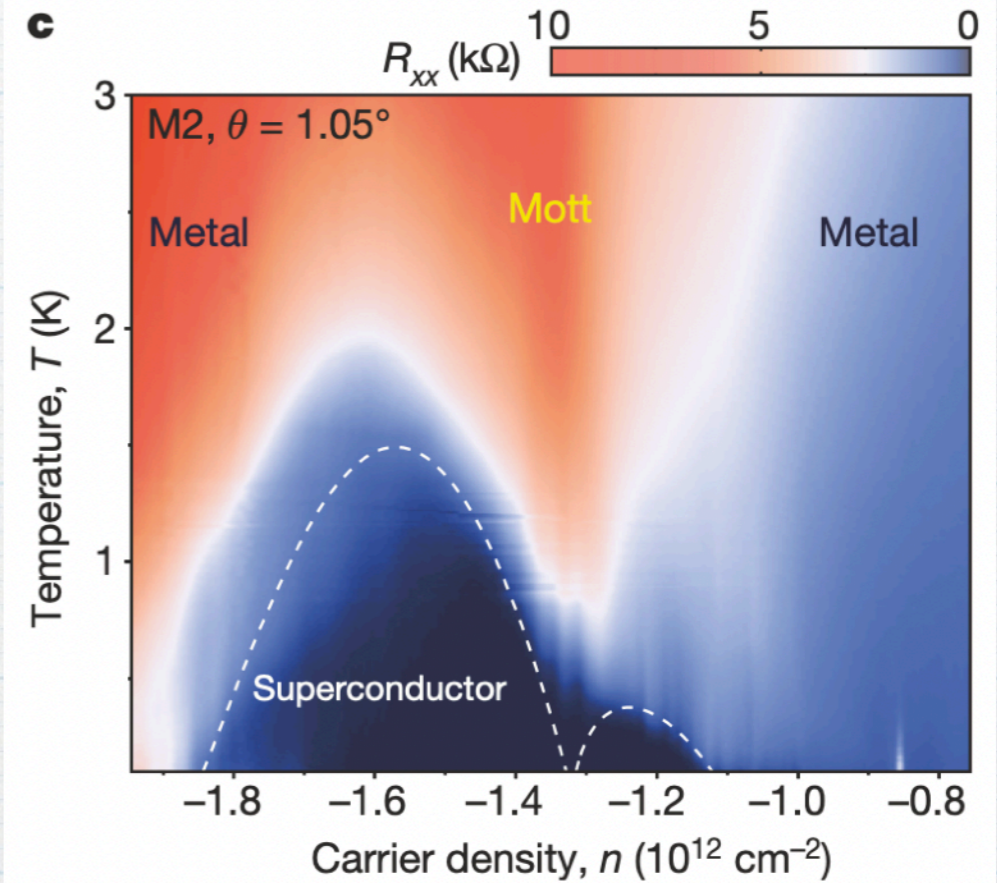
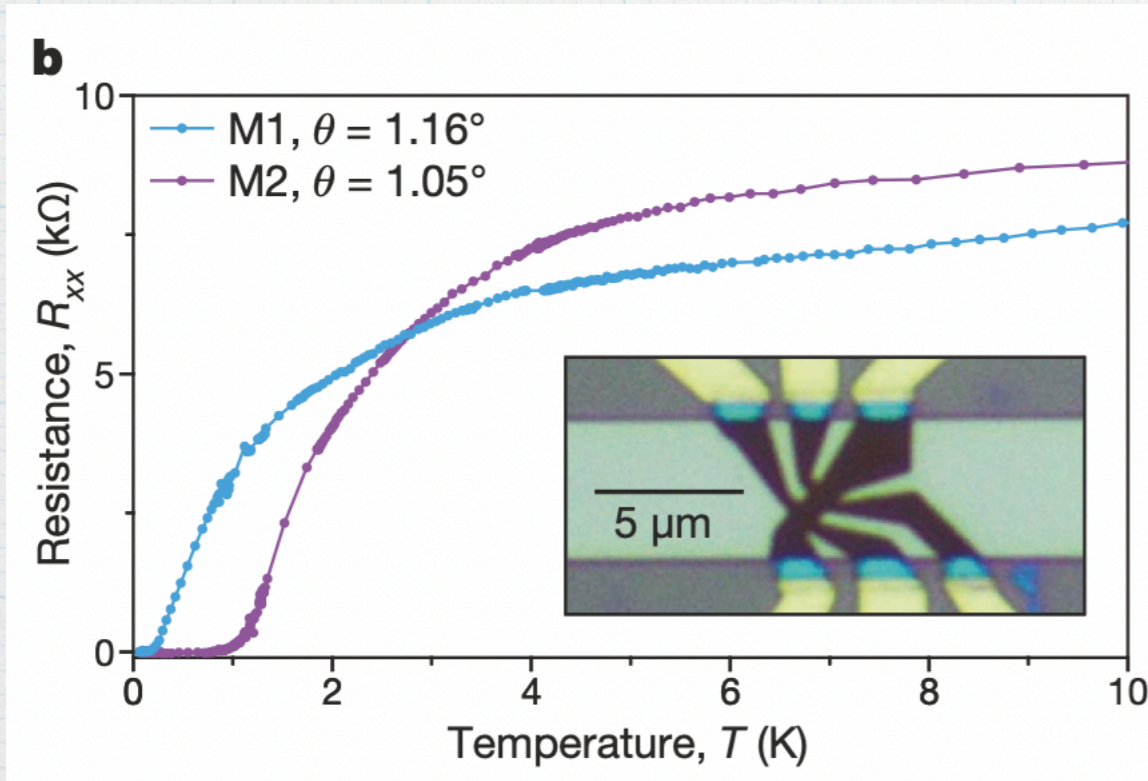
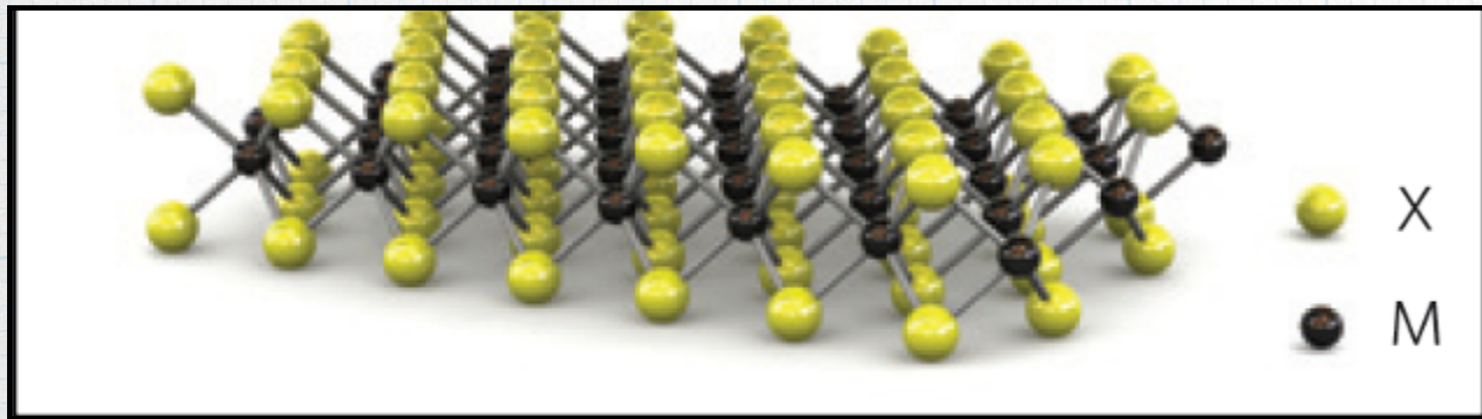


Fig. 4. Renormalized Dirac-point band velocity. The band velocity of the twisted bilayer at the Dirac point v^* is plotted vs. α^2 , where $\alpha = w/vk_\theta$ for $0.18^\circ < \theta < 1.2^\circ$. The velocity vanishes for $\theta \approx 1.05^\circ, 0.5^\circ, 0.35^\circ, 0.24^\circ$, and 0.2° . (Inset) The renormalized velocity at larger twist angles. The solid line corresponds to numerical results and dashed line corresponds to analytic results based on the eight-band model.

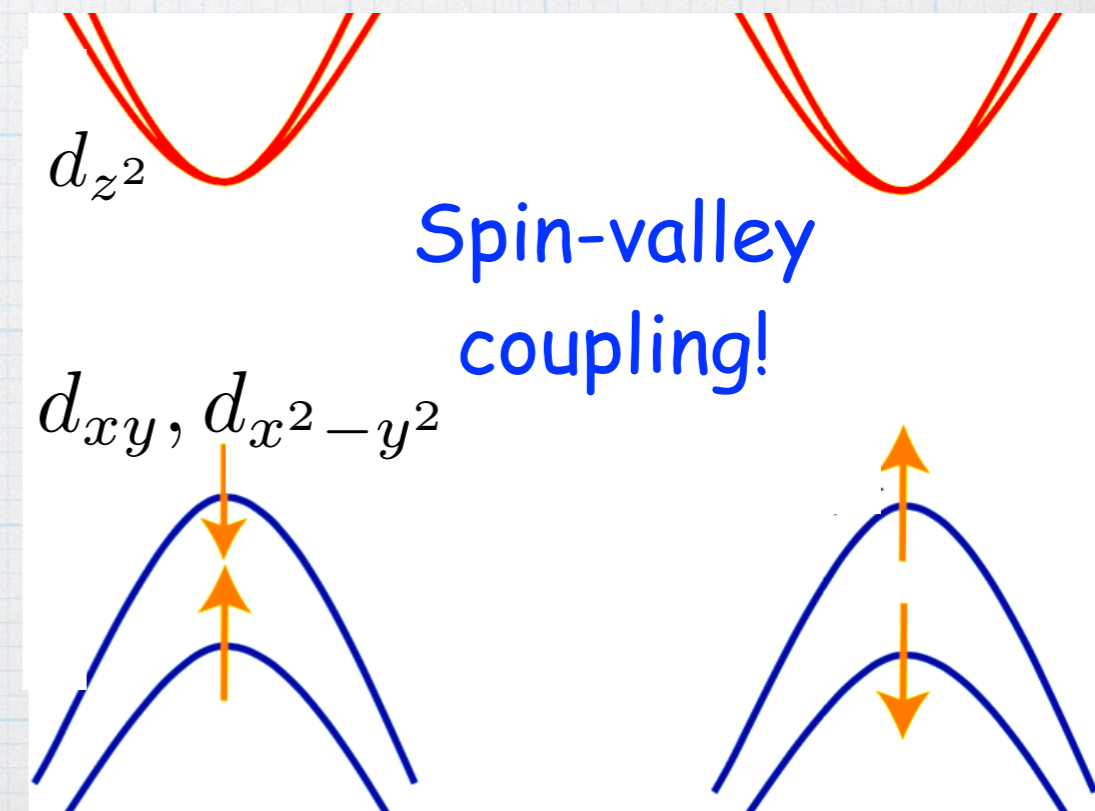
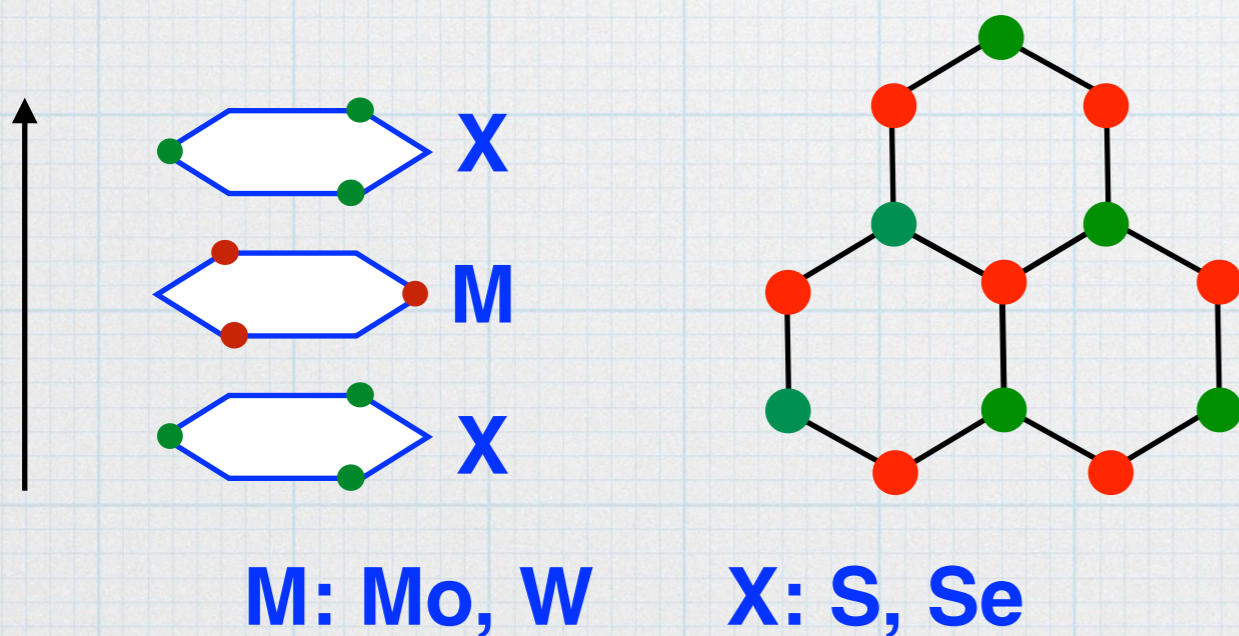
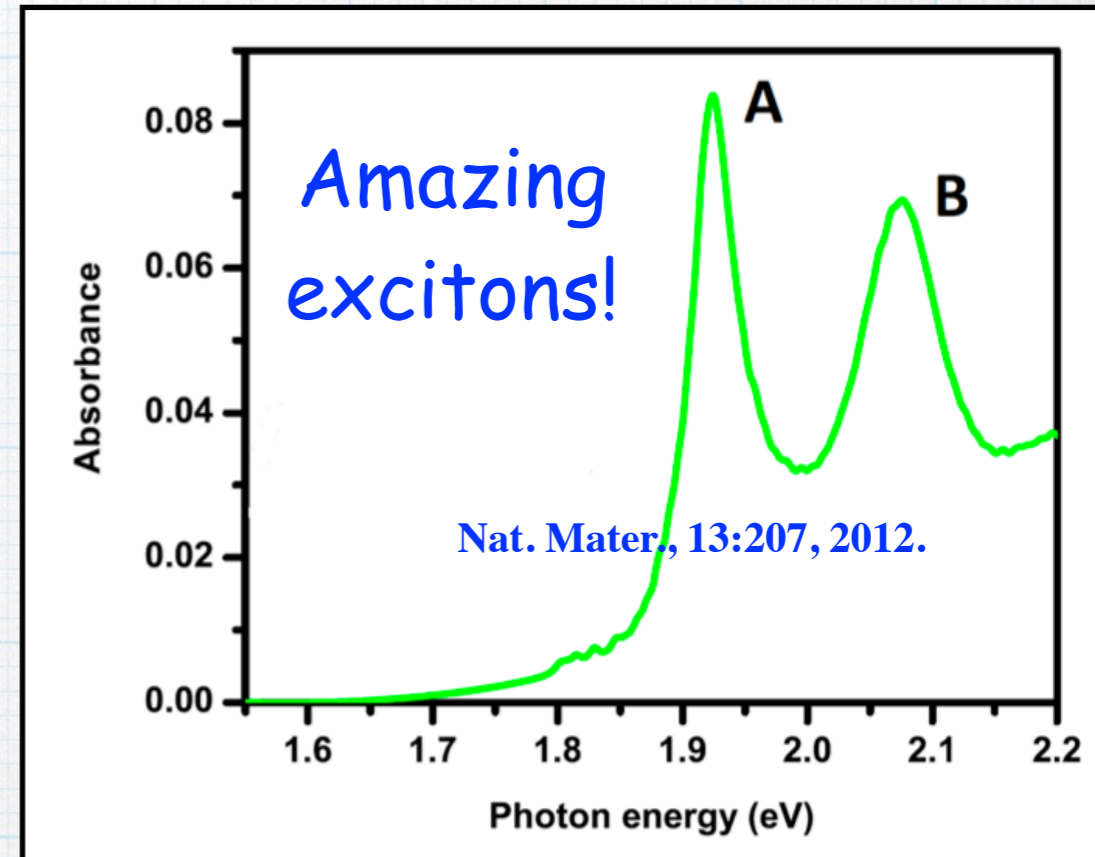
Y. Cao et al. Nature 556,80 (2018), Nature 556,43 (2018)



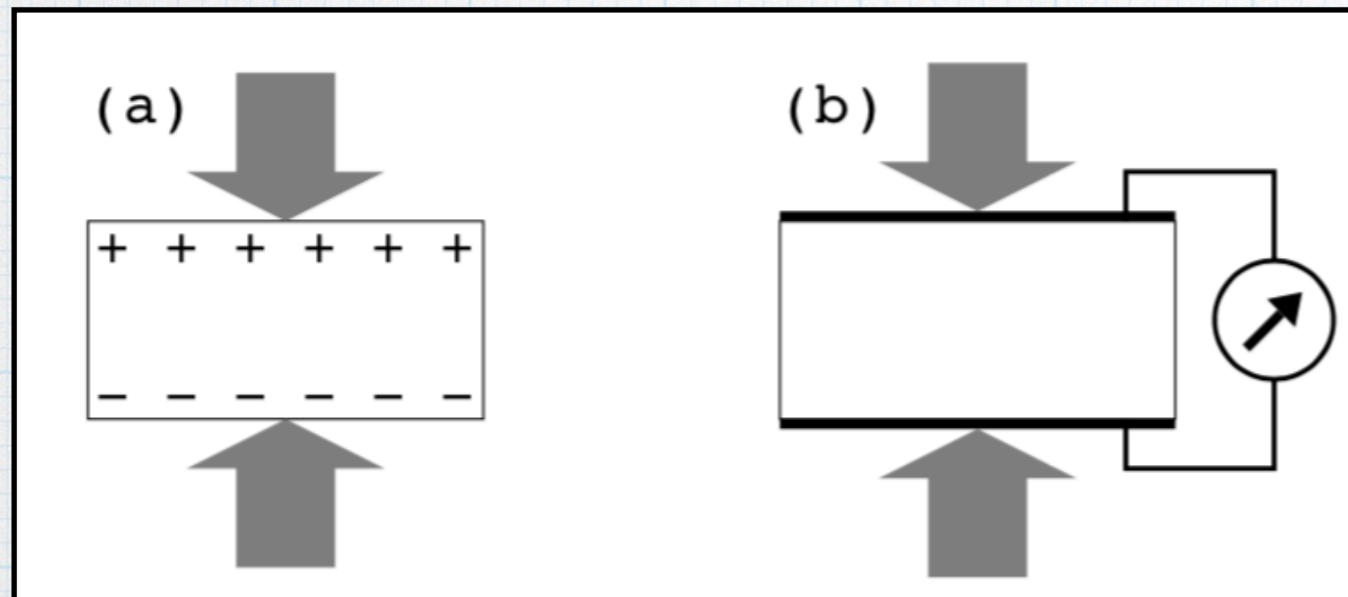
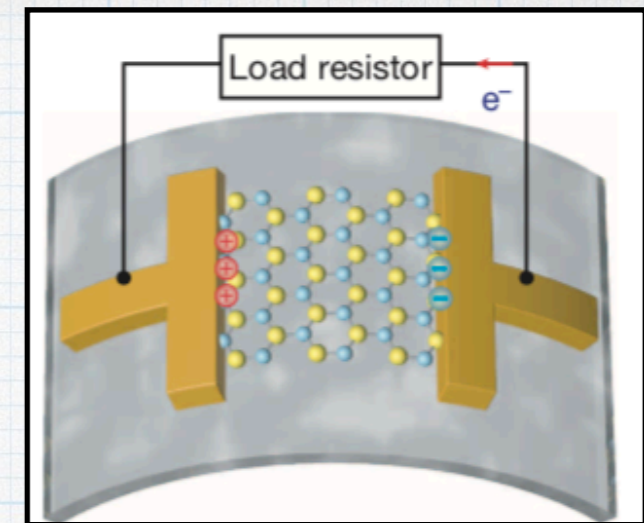
TMD: MoS₂, WS₂, ...



Nature Nanotech., 7:699, 2012.



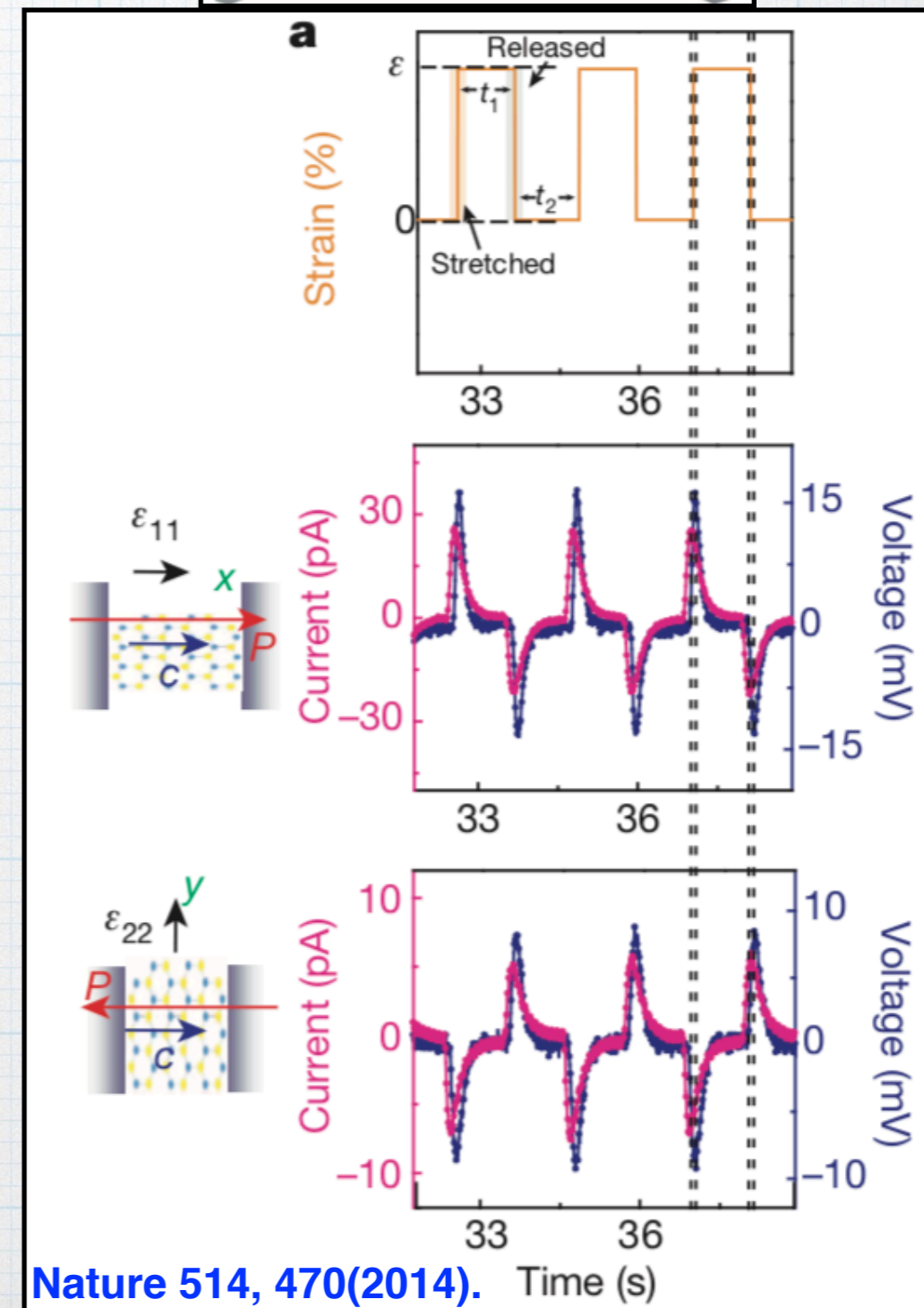
Piezoelectricity



$$P = \gamma : \epsilon$$

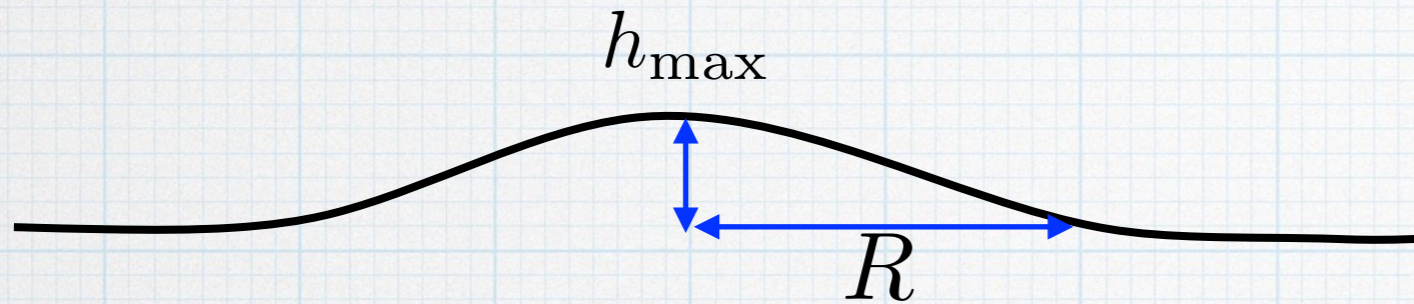
Piezo (pressure) \longrightarrow Electricity

$$j(t) = \partial_t P(t)$$



Induced density in circular bubbles

Nat. Comm 7, 12587 (2016).



$$\mathbf{P} = \gamma_{yyy} \mathbf{A} \times \hat{\mathbf{z}}$$

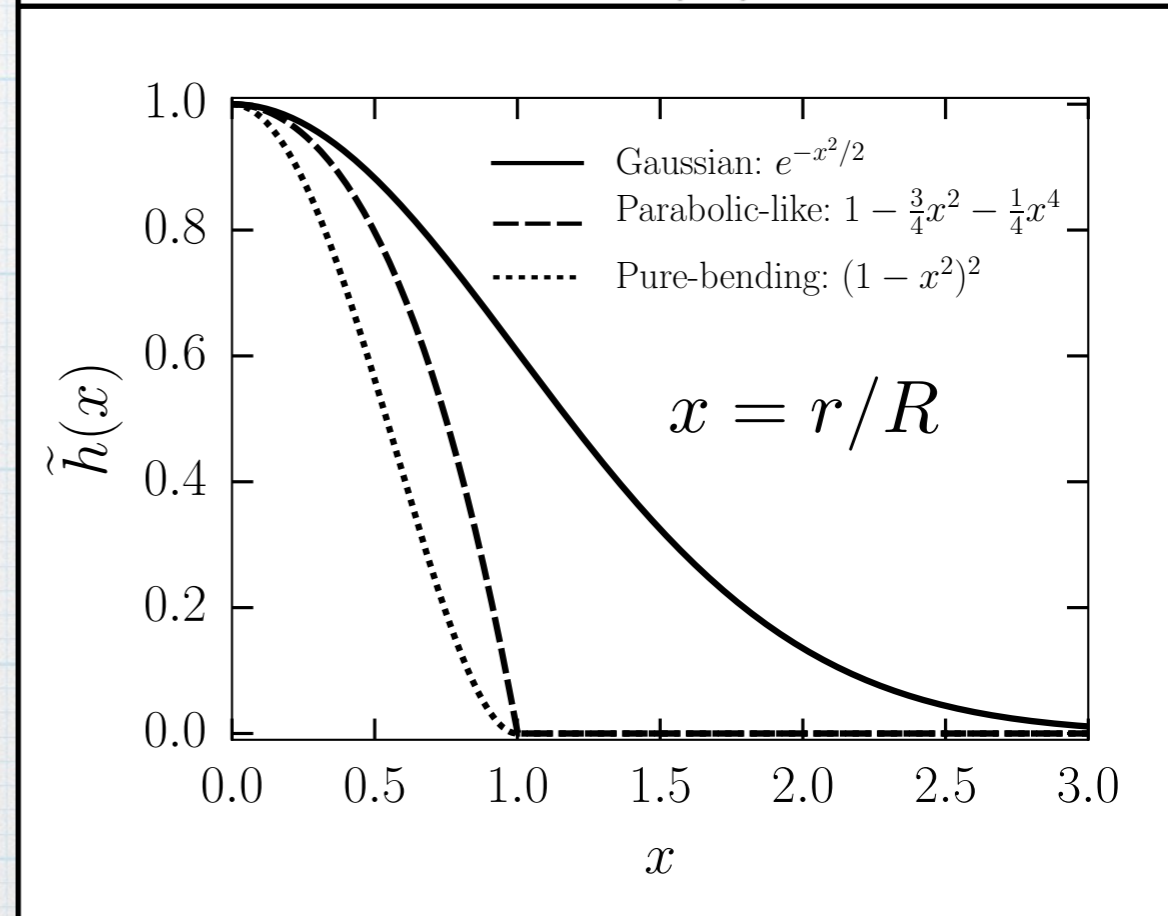
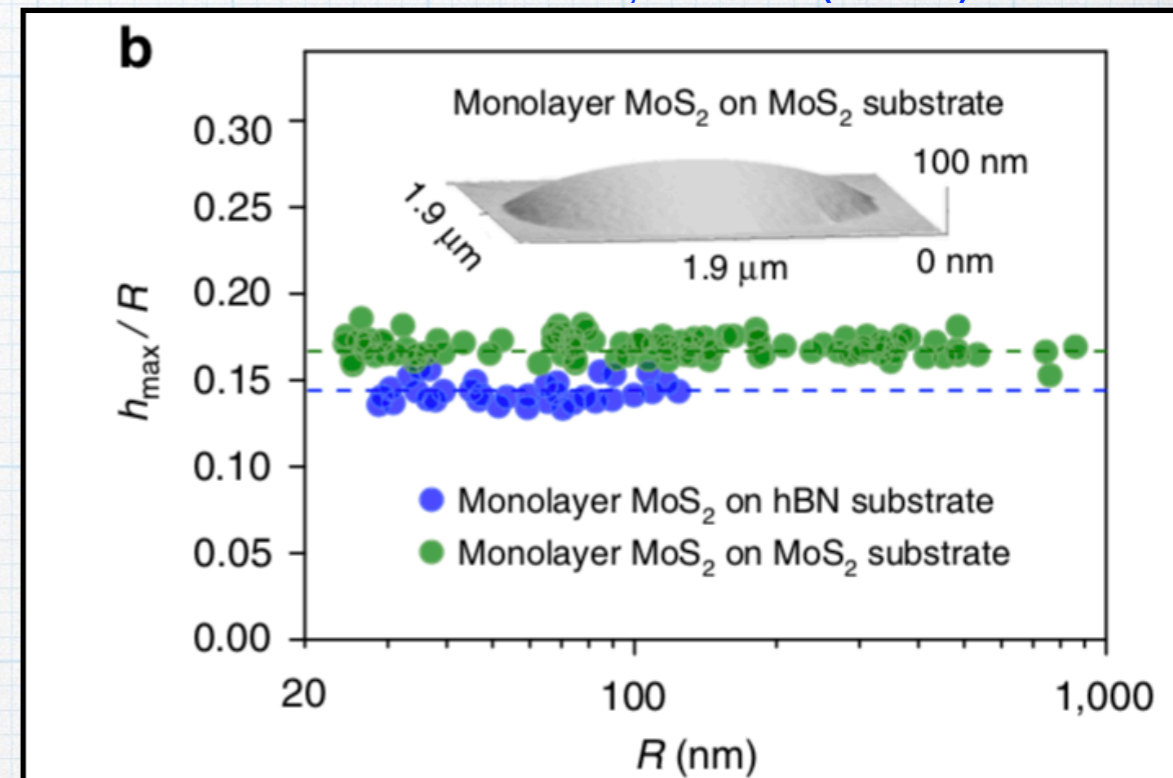
$$\mathbf{P}(\mathbf{r}) = p(r) [\hat{\mathbf{r}} \sin(3\theta) + \hat{\boldsymbol{\theta}} \cos(3\theta)]$$

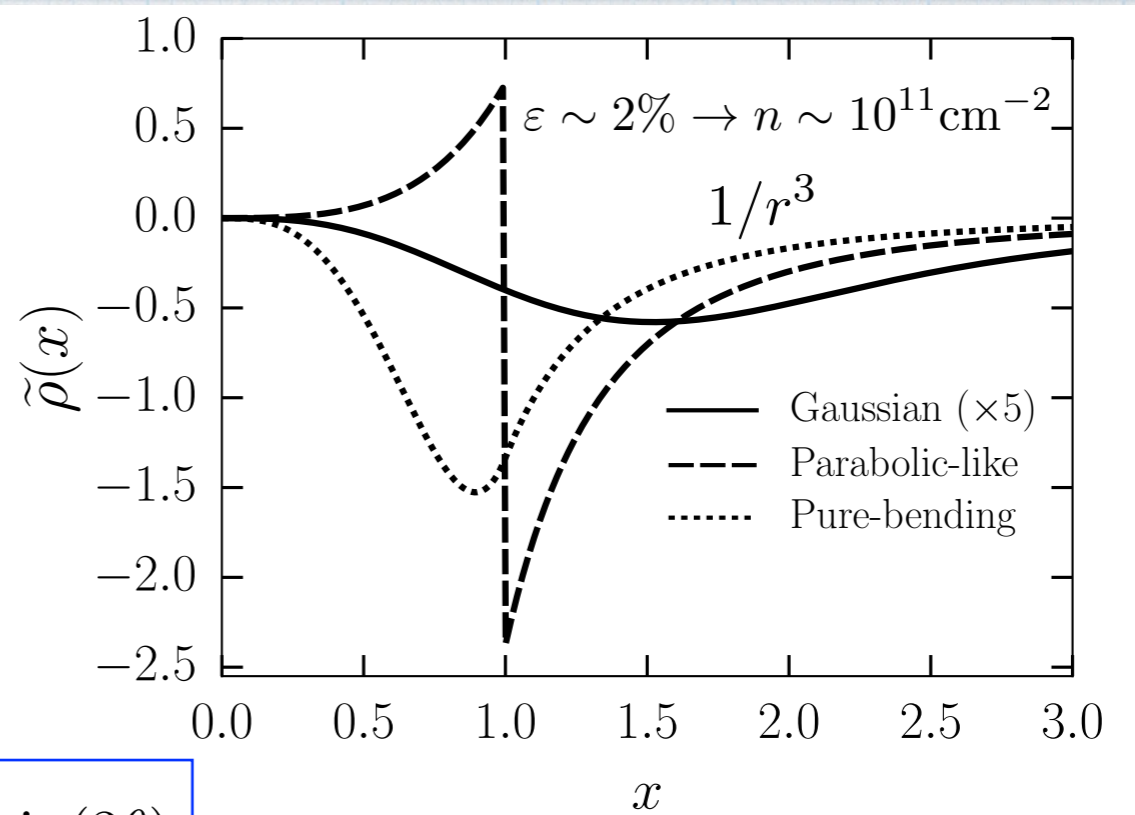
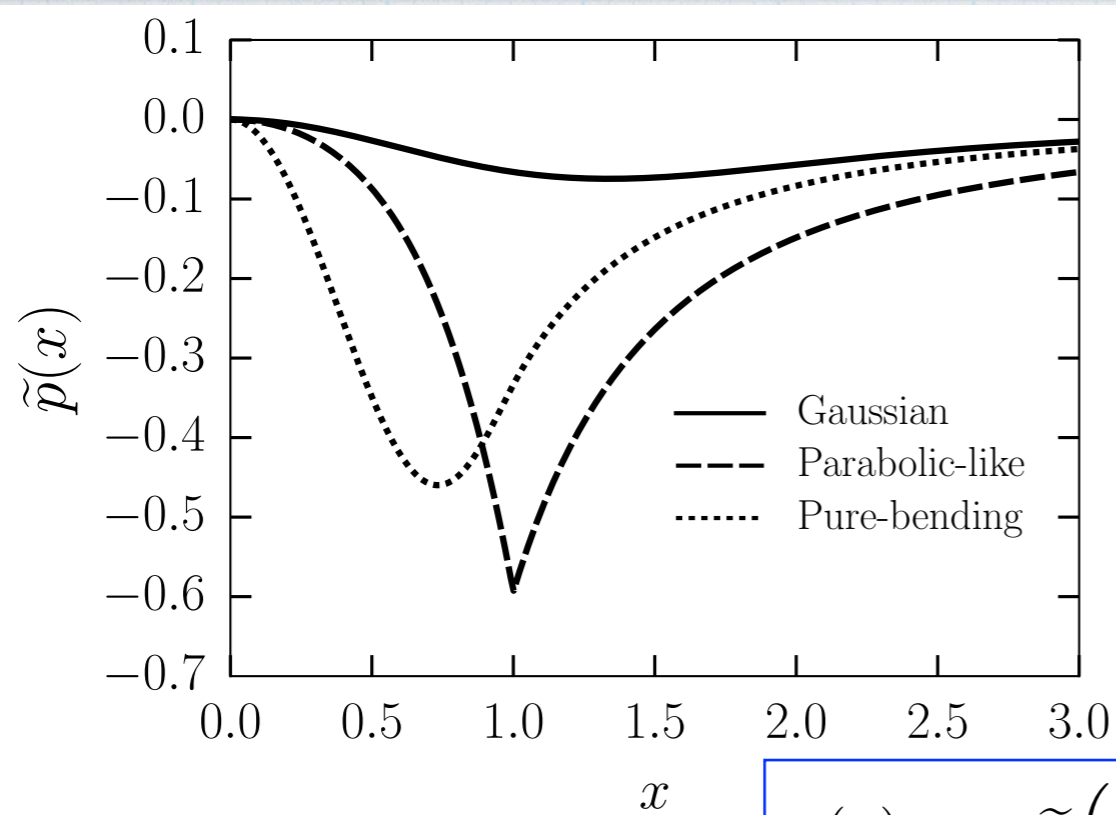
$$p(r) = \gamma \left\{ \frac{u(r)}{r} - \frac{\partial u(r)}{\partial r} - \frac{1}{2} \left(\frac{\partial h(r)}{\partial r} \right)^2 \right\}$$

$$\rho(\mathbf{r}) = -\nabla \cdot \mathbf{P}(\mathbf{r}) = -\gamma [\nabla \times \mathbf{A}(\mathbf{r})]_z$$

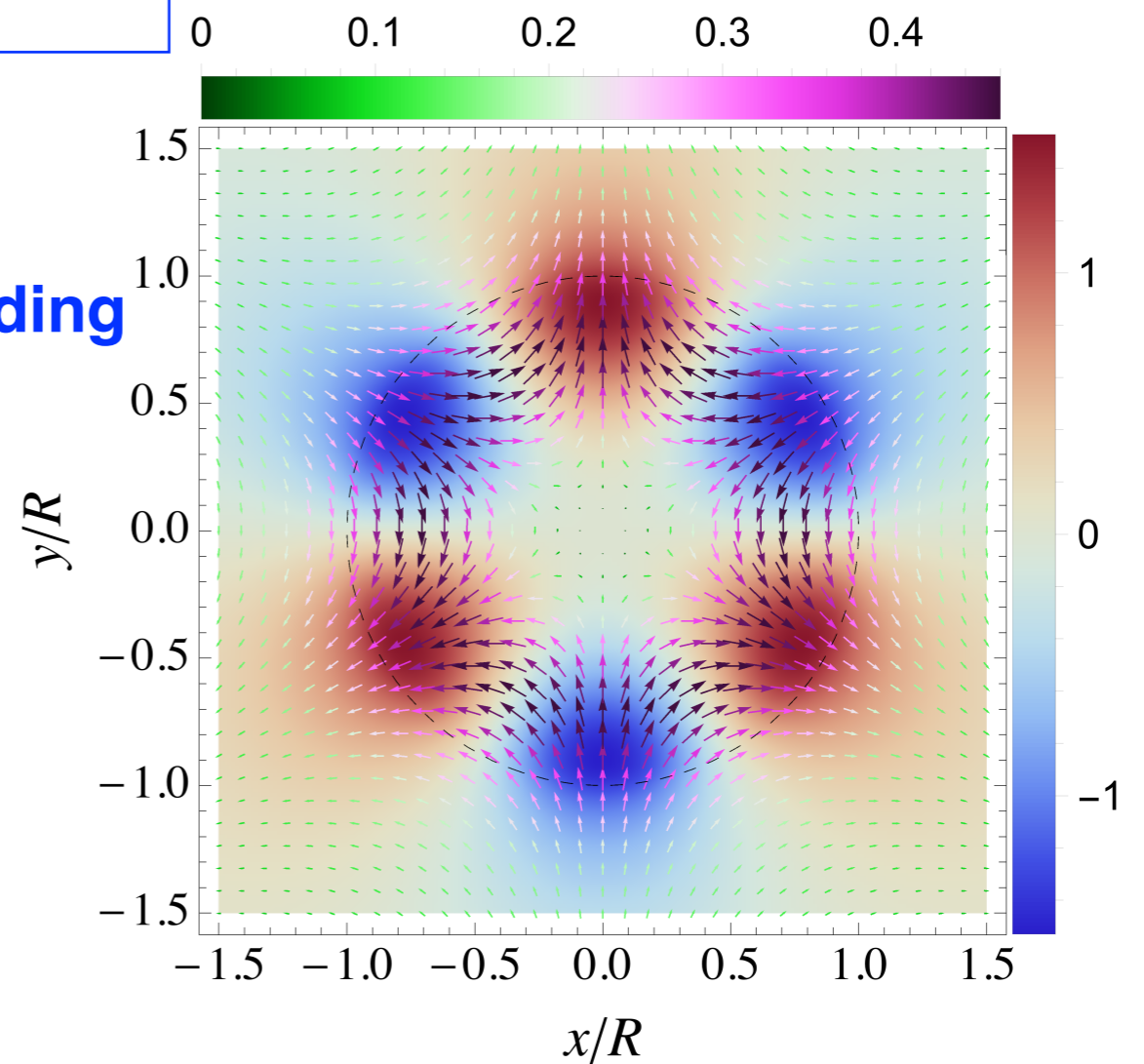
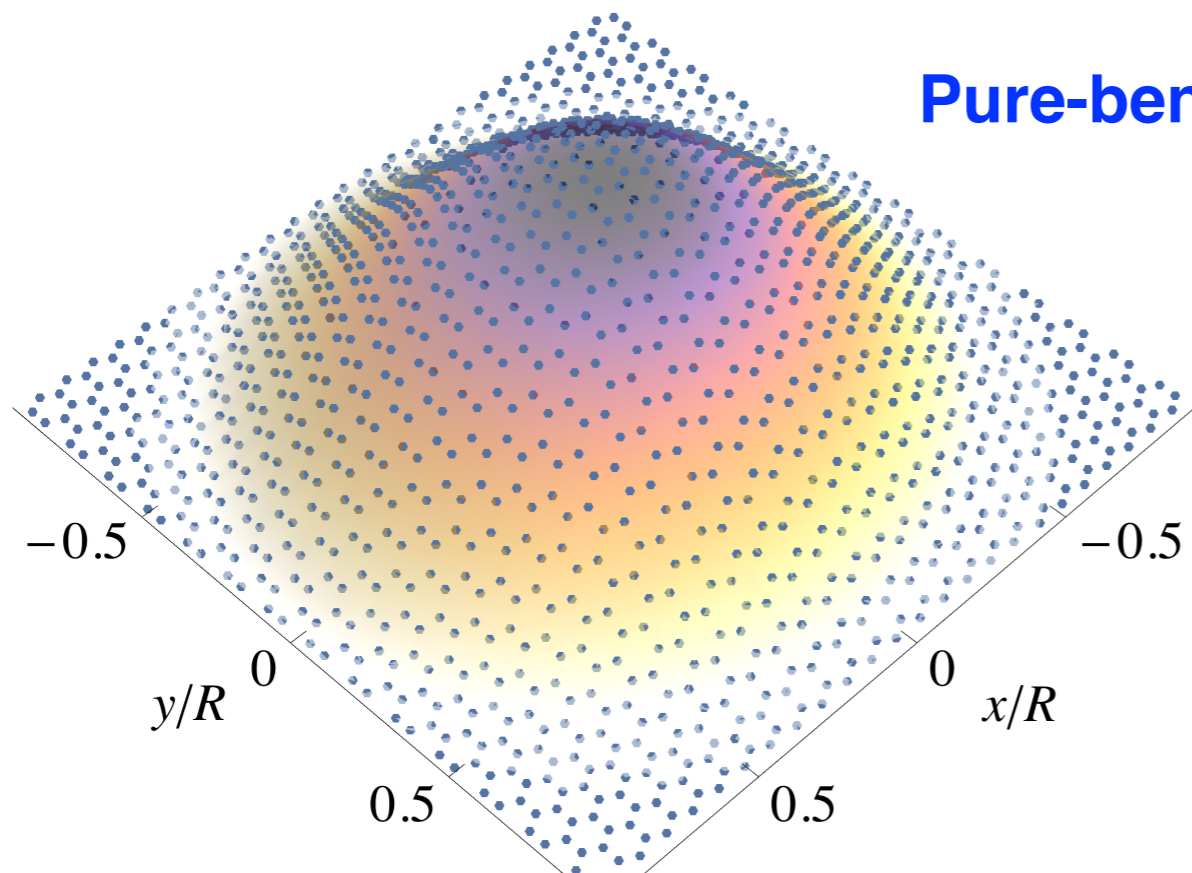
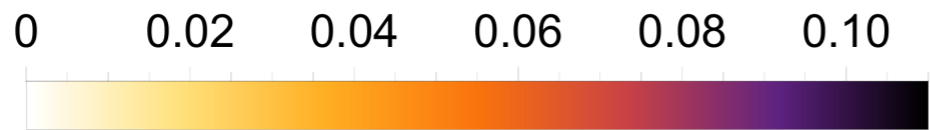
$$\rho(\mathbf{r}) = \left(\frac{p_0}{R} \right) \tilde{\rho} \left(\frac{r}{R} \right) \sin(3\theta)$$

$$p_0 = \gamma(1 + \nu) h_{\max}^2 / R^2$$





$$\rho(\mathbf{r}) = \rho_0 \tilde{\rho}\left(\frac{r}{R}\right) \sin(3\theta)$$



Summary

- A. van der Waals layered materials provide a rich platform for nano-kirigami (origami) technology and flexible optoelectronic
- B. 2D materials' electronic properties are highly sensitive to lattice deformation (strain): e.g. Pseudo Landau Levels
- C. Relative rotation (twist) can lead us to exotic strongly correlated phases in 2D material's heterostructure

Thank you